

Impacts of variable nutrient stoichiometry (N, Si, and P) on a coastal phytoplankton community from the SW Bay of Bengal, India

Debasmita Bandyopadhyay[#] and Haimanti Biswas*

CSIR National Institute of Oceanography, Biological Oceanography Division,
Dona Paula, Goa 403004, India.

[#] Present address: National Centre for Coastal Research (ICMAM PD),
NIOT Campus, Velachery, Tambaram Main Rd,
Pallikaranai, Chennai, Tamil Nadu 600100.

*Corresponding author email: haimanti.biswas@nio.org;
haimanti.biswas.nio@gmail.com

Abstract

The worldwide release of excessive nutrients [nitrogen (N), silicon (Si) and phosphorus (P)] into coastal waters is impacting phytoplankton growth and community structure. The coastal Bay of Bengal is predicted to be 90% more eutrophic in the future; the impacts on phytoplankton are largely unknown. We present the first experimental results concerning the responses of coastal phytoplankton to changing nutrient stoichiometry (N:Si:P) from the SW Bay. A gradual increase in Si, N and P supply resulted in exponential growth and significant nutrient depletion (Δ). The nutrients reaching the Bay are likely to possess a short residence time. We also show that any alteration in nutrient loading ratio may impact nutrient removal dynamics of N, Si and P differently. The growth saturating concentrations for Si, N and P were ≈ 55 , 65 and $10\mu\text{M}$, respectively, whereas luxury uptake was seen up to $20\mu\text{M}$ for P and $65\mu\text{M}$ for N and Si. Net consumption of N (ΔN) and P (ΔP) was decoupled from increasing Si levels. Gradual N enrichment under P- and Si-saturated conditions linearly increased ΔSi as well as ΔP , and diatoms dominated over cyanobacteria. *Thalassiosira* spp. seemed to respond positively to N enrichment, probably due to their high nitrate uptake and storage capacity, associated with the common occurrence of this species here. *Nitzschia* spp, a pennate diatom, showed the opposite trend. Such modifications may have direct consequences on the food chain. The rates of N, Si and P removal under the saturated levels were 1.03 ± 0.27 , 1.35 ± 0.14 and $0.14\pm 0.02\ \mu\text{mol Chl}a^{-1}\ \text{d}^{-1}$, respectively and yielded a ratio of 7.5:9.8:1 for N:Si:P. The projected departure from the Redfield ratio (eutrophication) in the Bay may potentially alter nutrient removal patterns, phytoplankton community composition and autochthonous organic matter stoichiometry.

Keywords: Phytoplankton; Diatoms; Bay of Bengal; Eutrophication; Redfield ratio; Nutrient stoichiometry; Nutrient uptake.

Introduction

Coastal phytoplankton communities remove a significant amount of dissolved inorganic carbon and nutrients from coastal waters and support coastal fisheries. In general, phytoplankton growth and community composition are largely controlled by three major inorganic nutrients, nitrogen (N), phosphorus (P), silicon (Si), and trace metals like iron (Tyrell, 1999; Amo & Brzezinski, 1999; Moor *et al.*, 2013). N is mainly utilized for synthesizing structural cellular materials (amino acids, nucleic acids, proteins) including enzymes, vitamins and pigments (Cira *et al.*, 2014). P is essential for synthesizing ATP, nucleic acids and lipids in all living cells (Brembu *et al.*, 2016). Si is mainly utilized by diatoms for siliceous frustule formation and diatoms contribute to removing up to 265×10^{15} mol silicon globally per annum (Yool & Tyrell, 2003).

The elemental ratio of carbon (C), N and P (106:16:1) in marine phytoplankton was found to be uniform throughout the deep sea, known as the Redfield ratio (Redfield, 1958) which was modified later as C:N:P:Si = 106:16:1:15 (Brzezinski, 1985). In the marine environment, not only the concentrations of these major nutrients control phytoplankton growth and community composition, but their ratios also play a key role. However, deviation from the classical Redfield ratio is frequently seen in coastal and marine waters (Martiny *et al.* 2013). Among phytoplankton, diatoms are the most efficient scavenger of nutrients in the aquatic environment (Lichtmann *et al.* 2007; Lomas and Gilbert, 2000). Hence, eutrophic marine systems like coastal seas and upwelling waters are usually occupied by diatoms and exhibit high primary productivity. Nevertheless, the internal nutrient storage capacity of phytoplankton is highly variable among different groups, genera and species of phytoplankton and this ability largely controls community shift in the natural environment.

In recent decades, natural N and P cycles have been considerably perturbed due to increasing anthropogenic activities in the water catchment areas (Rabalais *et al.* 2009). The usage of synthetic fertilizer enhanced N and P drainage (eutrophication) into coastal waters (Gilbart *et al.* 2014) all over the globe (Turner *et al.* 2006; Garnier *et al.* 2010; Gao & Zhang, 2010). Aquaculture in coastal areas has been identified as one of the major contributors of N and P and has been predicted to increase considerably (Bowman *et al.* 2011; Boesch, 2019). Conversely, the river-borne Si transport into coastal seas and estuaries decreased significantly due to increasing damming (Laruelle *et al.* 2009). On the other hand, accelerated land-use change is largely impacting Si loading in the coastal waters (Chen *et al.* 2014). Diatom growth and cell division rates are obligatory to Si availability; hence, interrupted Si supply may restrict diatom growth and could promote non-siliceous phytoplankton bloom (Davindson, 1999). A shift in phytoplankton community structure from a beneficial to harmful or a siliceous to non-siliceous bloom may occur due to the imbalances in N:P:Si ratio

(Turner *et al.* 2006; Smyda, 1990; Zhou *et al.* 2008). The rapidly changing nutrient stoichiometry, i.e., a departure from the Redfield ratio, may potentially impact phytoplankton growth, community composition and organic matter stoichiometry in coastal seas (Smyda, 1990; Conley & Malone, 1992; Piehler *et al.* 2004; Martiny *et al.* 2013).

A good example can be the North Sea (Burson *et al.* 2016) where Europe's progressive de-eutrophication efforts decreased overall P loading relative to N; this led to a major shift in phytoplankton community structure and growth. Palaeo records showed that in lower North American great lakes subsequent P enrichment after European settlements led to Si depletion due to massive biogenic silica (BSi) formation associated with diatom bloom (Schlske *et al.* 1983). Likewise, Martin *et al.* (2017) noticed a significant decrease in nitrogen fixing cyanobacterial bloom in the southwest coast of India over the last few decades associated with increased N and P inputs. Earlier studies established a strong correlation between phytoplankton stock, water quality and fisheries resources on the west coast of India (Subrahmanyam, 1958 and references therein) suggesting immediate consequences of phytoplankton community shift on planktivorous fish.

In India, the inputs of the river carried P to coastal seas is estimated twice as much as other rivers in the world (Ramesh *et al.* 2015). Increasing agricultural activities with the growing population of India is also enhancing N input (Ramesh *et al.* 2017) in coastal areas. The Coastal Bay of Bengal (BoB) receives a significantly large amount of nutrients from numerous rivers as well as via land runoff influenced by the summer monsoon. It was seen that N and P loadings in the Bay of Bengal have been increased by 35-40% within 1970 -2000 and were mostly related to agricultural activities. Moreover, with the growing population and agricultural practice, loads of N and P have been predicted to double by 2050 (Sattar *et al.* 2014). Furthermore, in this area, there has been a steady increase in the number of tropical cyclones (Balaguru *et al.* 2014) which may also enhance the nutrient supply and phytoplankton bloom in the surface waters (Girishkumar *et al.* 2019). Such modifications in nutrient stoichiometry may potentially impact coastal phytoplankton growth, community composition and the elemental ratio of autochthonous organic matter. The coastal BoB is usually dominated by diatoms (Bandyopadhyay *et al.* 2017 and references therein). A shift in phytoplankton community structure from a beneficial to harmful or a siliceous to non-siliceous bloom may occur due to the imbalances in N:P:Si ratio (Turner *et al.* 2006; Smyda, 1990; Zhou *et al.* 2008). There are several coastal water monitoring programs available from these regions and those studies may provide some ideas about seasonal shifts in the phytoplankton community. But, in an open system, it is difficult to link any observed trend to a particular variable (like altered nutrient stoichiometry), since the numbers of variables are often too many. Conversely, controlled

experiments provide the advantage of monitoring growth patterns/community shifts against one variable (e. g. a particular nutrient concentration) keeping other factors unchanged. Hence, experimental studies help to develop some ideas about future phytoplankton community response to the projected scenarios and also useful to formulate policies to tackle eutrophication for uninterrupted ecosystem services. Nevertheless, no experimental study has been done so far in this area showing the impacts of variable nutrient stoichiometry on phytoplankton growth, nutrient uptake potential and community composition.

In the present study, we have altered the major nutrient supply ratios in three independent experiments. For each experiment, one key nutrient level varied, whereas, the other two were supplied at saturated levels. It should be noted that such growth saturating nutrient concentrations are not frequently seen in the coastal Bay, but often reported from the large estuarine systems like Ganges and Godavari (Biswas *et al.* 2004; Mukhopadhyay *et al.* 2006; Biswas *et al.* 2010; Sarma *et al.* 2010). These studies were conducted over multiple years covering all seasons. The averaged Si concentration reported in the lower estuarine stretches from these studies was $60.2 \pm 13 \mu\text{M}$. This suggests that for the estuarine and coastal phytoplankton this is possible to experience such a high amount of Si. However, there is no such study that shows how such large quantities of nutrients are consumed by phytoplankton from this region. Further, under the projected eutrophication scenario in the coastal Bay, this is essential to understand the growth responses of phytoplankton at saturated nutrient levels (Gilbert *et al.* 2016) which may eventually lead to “luxury” uptake even under eutrophic condition. We also argue that a simple nutrient enrichment experiment just by altering the classical Redfield Ratio within average nutrient ranges may not provide the actual information on growth saturating and luxury nutrient consumption levels. Therefore, we had chosen the growth saturating nutrient levels to document the nutrient uptake potential of the phytoplankton from a coastal station (Visakhapatnam) of the SW Bay of Bengal. The observed growth responses, nutrient uptake and community shift trends are discussed in terms of different physiological parameters.

Materials and Methods

Stock culture

All polycarbonate (Nalgene, USA) bottles used in this study were acid cleaned followed by repeated MQ washes. The coastal waters were collected from the Visakhapatnam coast ($17^{\circ}42'108''$ N and $83^{\circ}19'064''$ E) (Fig. 1) ($\approx 1\text{m}$ depth) with the help of a clean plastic beaker into two 20L bottles and pre-filtered with a $200\mu\text{m}$ zooplankton mesh (to reduce grazing pressure by large mesozooplankton). To develop the stock culture, an aliquot of seawater was transferred into a 4L bottle and N, Si and P

were added in the form of nitrate (KNO_3 , Merck, Germany) silicate (Na_2SiF_6 , Sigma, USA) and phosphate (KH_2PO_4 , Merck, Germany), respectively ($100 \mu\text{M NO}_3$; $100 \mu\text{M SiO}_3^{-2}$; $20 \mu\text{M PO}_4^{-3}$). This water was equally distributed in two bottles and incubated inside a water bath under a natural day-night cycle (12:12 hours) on an open terrace. The water bath was screened with a nylon mesh to mimic the light penetration at 1m water depth (for details please see Biswas *et al.* 2017). The water in the bath was exchanged repeatedly to maintain the average temperature of $\approx 28^\circ\text{C}$ which is usually seen in the coastal BoB. Every day the bottles were mixed gently (without taking them out of the mesh) with care at a particular time of the day to avoid any sedimentation of biomass at the bottom. After 48hrs of incubation, dense diatom biomass formation was noticed and this culture was used as a stock culture for the main experiments. Please note that the stock cultures were not the same for all experiments and were grown following the same protocol before the individual experiment. The initial nutrient concentrations were also quite different at the time of collecting seawater and are mentioned in the following sections. The rest of the water (40L) was filtered using GF/F filters (Advantec, Japan) followed by $0.22\mu\text{m}$ filters (polycarbonate membrane, Millipore) to screen all other biomass and kept for the main experiment. Just before commencing the individual experiment, nutrients (N, P and Si) were added in different ratios and initial biomass was maintained at low concentrations ($<0.5\mu\text{g L}^{-1}\text{Chl}a$).

Experimental planning

Altogether, three experiments (Fig. 2) were conducted during this study. The main experiments were incubated for 72 hours. The added nutrient concentrations were chosen based on the trial experiments that were conducted before the main experiments to know the approximate saturation levels of N, Si and P. It was observed that for each nutrient, after the growth saturating levels, further nutrient additions didn't impact nutrient depletion or growth. These particular nutrient levels [for N and Si this was $100\mu\text{mol L}^{-1}$ and for P $\approx 20\mu\text{mol L}^{-1}$] were chosen for setting the experiments. The details of the individual experiment are discussed below.

Experiment I

The first experiment addressed the impacts of variable Si supply on phytoplankton growth under unaltered N and P levels. During the time of water collection, the concentrations of N, Si and P were $6.91\mu\text{M}$, $9.57\mu\text{M}$ and $1.15 \mu\text{M}$, respectively. This experiment was conducted in two sub-sets; in the first set (Exp-IA), N and P levels were five times higher than the second set (Exp-IB). The details are discussed in the following section.

Exp-IA

In a 20L bottle containing pre-filtered seawater, 100 μ M N and 20 μ M P (final concentrations) were added and mixed thoroughly before distributing in seventeen 1 L bottles. Si stock was added to make the final concentrations from 20 - 200 μ M. An equal amount of phytoplankton biomass (5 mL) was added to each bottle from the stock culture.

Exp-IB

In another 20L bottle (Nalgene, USA), 20 μ M N and 4 μ M P were added to the sterile filtered seawater and were evenly distributed in seven 1 L bottles (acid cleaned; Nalgene, USA). Si stock was added to each bottle to make the final concentrations of 10 to 200 μ M Si (7 sets). An equal amount of phytoplankton biomass was added to each bottle from the stock culture. A similar protocol was followed for each experiment as described for the stock-culture.

Experiment II

The second experiment (Exp-II) examined the growth responses of phytoplankton to variable P supply under unaltered N and Si concentrations. During this experiment, the initial nutrient concentrations were as follows: N =11.26 μ M; P =1.9 μ M; Si =7.68 μ M. Another 20L bottle filled with the pre-filtered coastal water was enriched with 100 μ M Si and 100 μ M N and evenly distributed in fifteen 1L bottles after thorough mixing. P levels varied from 2.5 μ M to 20 μ M (final concentrations). An equal amount of stock culture was added to each bottle and incubated under the same condition as mentioned earlier. In addition to Chl*a* and BSi estimation, HPLC pigments were also analyzed for this experiment. Random microscopy was done to check the stock culture before setting the experiment.

Experiment III

The third part of this experiment monitored the growth response and nutrient uptake potential in coastal phytoplankton under variable N levels and fixed Si and P levels. During this experiment, the initial N level was 14 μ M and additional N was added (24, 34 and 64 μ M) in the presence of unaltered Si (100 μ M) and P (10 μ M) levels. Since we had only four N levels, replicates were there for each treatment. In addition to Chl*a*, BSi and nutrients, total protein, HPLC pigment and microscopic analyses of the phytoplankton community were also done.

Analytical methods

All dissolved inorganic nutrients were analyzed by using the spectrophotometric (Shimadzu UV-VIS-1800) method following the standard protocol of Strickland and Person (1972). N represents nitrate+nitrite. Ammonia was not measured. Net nutrient depletion or uptake (Δ) was quantified by

subtracting the final nutrient values from its initial level. For quantifying Chlorophyll *a* (Chl*a*), a 100-200mL water sample was filtered onto a GF/F filter (25mm, Advantech, Japan) using a vacuum pump (Rocker 600) (pressure < 200mmHg) under the low light condition to avoid photo-bleaching. Filters were folded in the quarter and kept inside an aluminum wrap at -20°C. Prior analysis, filters were soaked in 3-5mL of 90% ice-cold acetone (HPLC grade, Merck, Germany) in a brown glass vial and kept tightly closed overnight at -20°C for extraction. Next day fluorescence values of the samples were measured using a Fluorometer (Carry Eclipse, Varian) against the standard Chl*a* solution (Sigma Aldrich, USA). Chl*a* based specific growth rate was calculated using the final and initial Chl*a* values using the following formula:

$$\text{Specific growth rate } (\mu_{\text{Chl}a} \text{ d}^{-1}) = [\ln(\text{final Chl}a) - \ln(\text{initial Chl}a)] / \text{number of days.}$$

For quantifying biogenic silica (BSi), a 100mL subsample was filtered onto a 0.2µm black polycarbonate membrane (GTTP, 47mm, Millipore) and stored by folding in quarter inside a plastic Petri-plate at 4°C until analysis. Prior analysis, the filters were oven-dried at 60°C and then hydrolyzed in 5mL 2N NaOH solution at 100°C in a temperature-controlled water bath for one hour. After removing the samples from the water bath the solutions were neutralized with 5mL of 2N HCL. From this mixture, 1mL of supernatant was taken in a plastic tube and made the volume up to 25mL with MQ water. Dissolved Si was estimated by using the standard protocol as stated above. Total protein was quantified following the Lowry's colorimetric method (Lowry *et al.* 1951) using Folin-Ciocalteu's solution. For phytoplankton pigment analysis, the filters were soaked in 3 -5 mL of ice-cold 90% acetone (HPLC grade from Merck Chemicals) in amber glass vials overnight at -20°C followed by homogenization (Ultra Turrax, Germany) and centrifugation (-10 °C) (Eppendorf, Germany). The supernatant was used to quantify phytoplankton pigments using an HPLC (Agilent Technology; Series 1200, C8 column, pore size 3.5mm and a photodiode array detector) following the method of Heukelem and Thomas (2001). The contribution of different size classes (micro, nano, picophytoplankton) of phytoplankton (based on the concentrations of Chl*a* associated with different size class) was calculated from HPLC pigment data (Vidussi *et al.* 2001) using the following formula:

$$\text{Micro (\%)} = [\{1.4(\text{fucoxanthin}) + 1.4(\text{peridinin})\} / \text{DP}_w] \times 100$$

$$\text{Pico (\%)} = [(1.01(\text{chlorophyll } b) + 0.86(\text{zeaxanthin})) / \text{DP}_w] \times 100$$

(DP)_w = Diagnostic pigment was calculated using the following formula:

$$(\text{DP})_w = \sum (0.86) \text{ zeaxanthin} + (1.01) \text{ chlorophyll } b + (0.60) \text{ alloxanthin} + (1.27) 19'\text{-hex fucoxanthin} + (0.35) 19'\text{-but fucoxanthin} + (1.41) \text{ fucoxanthin} + (1.41) \text{ peridinin.}$$

Statistical analysis was performed using both way and single way ANOVA (at 95% confidence level; $p < 0.05$) in the Microsoft excel 2007 version. Linear regression analysis was done in Microsoft excel 2007 version.

Results

It should be noted that all experiments were conducted in diluted batch cultures and, always started from very low biomass. This method gives the best result for monitoring phytoplankton growth. The experiments with the natural community often get disturbed due to the interferences of grazers, allochthonous organic matter and simultaneous regeneration of nutrients within the experimental enclosures. These factors may collectively perturb the actual nutrient uptake and growth patterns. However, after 72 hours, phytoplankton biomass increased noticeably coupled with nutrient depletion in all treatments. The results of individual experiments are described in the following sections.

Experiment I

Exp-IA

As expected, Si addition showed considerable impacts on phytoplankton growth. The community was mostly dominated by the chain-forming centric diatom *Chaetoceros* spp; however, the community composition data are not presented here due to lack of reproducibility. Chla concentrations (Fig. 3a) and specific growth rates ($\mu_{\text{Chla}} \text{ d}^{-1}$) (Fig. 3b) showed a linear increase ($p < 0.01$) with increasing Si level from 20 μM to 55 μM and became non-linear after that (60 -200 μM Si). The increase in BSi contents (Fig. 3c) were tightly coupled with external Si supply ($p < 0.01$). BSi concentration at the 55 μM Si treatment was more than 3 times higher than that noticed at the 20 μM Si level (19.8 $\mu\text{mol L}^{-1}$). The ratios of BSi:Chla increased exponentially (Fig. 3d) with increasing Si supply ($R^2 = 0.65$; $p < 0.01$). Si uptake (ΔSi) (Fig. 3e) showed a significant linear correlation with increasing Si supply up to 65 μM ($R^2 = 0.64$; $p > 0.01$) and the magnitude of enhancement reached a plateau at 150 μM Si. ΔN (Fig. 3f) was inversely correlated with increasing Si supply ($p < 0.05$). ΔP concentrations were highly nonlinear with Si levels (Fig. 3g) indicating that P uptake was not directly dependent or controlled by Si supply. The ratios of $\Delta\text{Si}:\Delta\text{N}$ (Fig. 3h) showed an exponential increase ($R^2 = 0.88$; $p < 0.001$) with increasing Si concentrations and were likely to be influenced by Si rather than N uptake. Likewise, the ratios of $\Delta\text{P}:\Delta\text{N}$ (Fig. 3i) and $\Delta\text{Si}:\Delta\text{P}$ (Fig. 3j) were also significantly correlated with external Si levels.

Exp-IB

In this experiment, the concentrations of N and P were five times lower than Exp-IA. Here also a positive growth response was noticed with increasing Si addition. A linear increase in Chla content

was observed ($R^2 = 0.891$; $p < 0.05$) with increasing Si supply up to $60 \mu\text{M}$ (Fig. 4a) and this trend disappeared ($R^2 = 0.001$) after further Si addition. The specific growth rate varied from 0.97 to 1.32 and showed an exponential increase up to $60 \mu\text{M}$ Si addition (Fig. 4b). After this level, the correlation became insignificant with increasing Si. BSi contents (Fig. 4c) and BSi:Chl*a* ratios (Fig. 4d) enhanced exponentially ($R^2 = 0.881$; $p < 0.01$) with increasing Si levels. Net Si uptake (ΔSi) (Fig. 4e) was well correlated with Si concentrations and ΔN or ΔP uptake did not show any significant correlation ($P > 0.05$) with Si levels (Fig. 4f, 4g). The ratios of $\Delta\text{Si}:\Delta\text{N}$ was significantly correlated with Si concentrations (Fig. 4h); whereas, $\Delta\text{P}:\Delta\text{N}$ ratio (Fig. 4i) did not show any such trend. $\Delta\text{Si}:\Delta\text{P}$ ratios (Fig. 4j) were well correlated with Si concentrations. The trends of growth and nutrient uptake from Exp1A and Exp1B were compared in Fig. 5 to understand if there was any impact of different N and P supply on Si induced growth response. Surprisingly, the correlations between ΔSi (Fig. 5a; 5b), BSi contents (Fig. 5c, 5d), Chl*a* contents (Fig. 5e), and BSi:Chl*a* ratios (Fig. 5g, 5h) with increasing Si supply from Exp-IA and IB were insignificant.

Experiment II

Increasing P addition showed considerable impacts on phytoplankton growth dynamics. Very high P uptake potential was noticed. The concentrations of Chl*a* (Fig. 6a) increased significantly ($R^2 = 0.63$; $p < 0.001$) with increasing P supply. The highest Chl*a* concentration occurred at $9.9 \mu\text{M}$ P level and the concentration decreased slightly after further P enrichment. Chl*a* based growth rate (Fig. 6b) showed an exponential increase and was always > 1 in all treatments. BSi concentrations (Fig. 6c) were positively correlated ($R^2 = 0.57$; $p < 0.05$) with P levels and reached its maximum value at $9.9 \mu\text{M}$ P treatment followed by a plateau. The ratios of BSi: Chl*a* (Fig. 6d) did not show any clear trend with increasing P levels indicating that probably the magnitude of enhancement was similar for both the parameters. ΔP showed good linearity ($R^2 = 0.96$; $p < 0.001$) with P concentrations (Fig. 6e). ΔSi also showed a significant linear positive relation with P levels (Fig. 6f) ($R^2 = 0.763$; $p < 0.05$) up to $9.9 \mu\text{M}$; however, became nonlinear beyond this level (Fig. 6g). The ratios of $\Delta\text{P}:\Delta\text{Si}$ showed a significant positive correlation with P levels (Fig. 6h). BSi concentrations and ΔSi values were very well correlated.

HPLC pigment analyses showed the presence of five major diagnostic pigments [fucoxanthin (Fuco), chlorophyll *c*₂ (Chl *c*₂), diadinoxanthin (DD), diatoxanthin (DT) and β -carotene] representing diatoms. In addition to that, a negligible amount of zeaxanthin (Zea) was also detected. The concentrations of total pigments (TP) (Fig. 7a), Fuco (Fig. 7b), Chl*c*₂ (Fig. 7c), DT+DD (Fig. 7d) and β -carotene (Fig. 7e) showed an interesting trend with increasing P addition. Except for Chl*c*₂ (Fig.

7c), the other four pigments showed an exponential increase within 2.4 -4.4 μ M levels. Further P enrichment exhibited insignificant impacts on growth. The insignificant correlation between P levels and Chl_{c2} showed that chlorophyll synthesis was not directly influenced by P addition. The concentrations of Zea were very low (Fig. 7e) compared to Fuco, indicating the dominance of diatoms. Likewise, based on the diagnostic pigment concentrations, the contribution of microphytoplankton (Fig. 7f) showed dominance (>98%) over picophytoplankton (Fig. 7g) which represented less than 1% of the community.

Experiment-III

Increasing N supply revealed a significant impact on the growth and community structure of coastal phytoplankton. Chl_a concentrations (Fig. 8a), specific growth rate (Fig. 8b) and the concentrations of total protein (Fig. 8c) and BSi (Fig. 8d) increased with increasing N additions ($p < 0.05$). The ratios of BSi:Chl_a (Fig. 8e) showed an exponential negative correlation with increasing N levels suggesting that the relative enhancement in Chl_a was significantly higher than BSi production. Δ N concentrations showed high linearity with N levels (Fig. 8f). Δ P (Fig. 8g) and Δ Si (Fig. 8h) increased in response to increasing N supply. The ratio of Δ N: Δ Si (Fig. 8i) showed an exponential increase with increasing N level. This observation suggested that Δ Si increased when the N supply enhanced. A positive exponential trend was noticed with increasing N levels and Δ P: Δ Si uptake (Fig. 8j).

HPLC pigment analysis showed that Fuco was the major (>95%) diagnostic pigment with very little quantity of Zea. Additionally, Chl_{c2}, DT + DD and β -carotene were also detected. The concentrations of total pigment (TP) (including Chl_a) (Fig. 9a), Fuco (Fig. 9b), Chl_{c2} (Fig. 9c), DD+DT (Fig. 9d), β -carotene (Fig. 9e) and Zea (Fig. 9f) showed an exponential increase with increasing N supply. However, the magnitude of increase in chlorophyll contents (Chl_a and Chl_{c2}) in response to increasing N supply was higher than that of carotenoids. Based on the diagnostic pigments, phytoplankton community composition was configured and the results showed that Fuco containing microphytoplankton (Fig. 9g) contributed almost 95 - 98% of the community and showed exponential growth enhancement with increasing nitrogen supply. Zea containing picophytoplankton contributed to < 5% of the community (Fig. 9h) and decreased exponentially with increasing nitrogen supply. Microscopic analysis of the phytoplankton community in terms of relative abundance is presented in Fig. 10. The initial community (stock culture) was dominated by the centric diatoms, *Thalassiosira* spp. (36%) and *Chaetoceros* spp. (10.6%) along with pennate diatoms *Nitzschia* spp. (\approx 40%) and *Thalassiothrix* spp. (3.3%). Over the experimental period, the community structure changed significantly. Increasing N addition also impacted the community composition

significantly. The relative abundance of *Thalassiosira* spp. was 12% in the first treatment and increased exponentially with increasing N supply and contributed almost 75% of the community in the highest added N level. The abundance of *Nitzschia* spp. varied within the first three N levels without any statistical significance ($\approx 30\%$) and decreased to half at $64\mu\text{M}$ nitrate level. In this treatment, *Chaetoceros* spp. showed 3 times higher values than its initial abundance; however, decreased to $<2\%$ under the highest N level. *Thalassiothrix* spp. decreased gradually from its initial abundance (3.4%) and became $<1\%$ at the highest nitrate level.

To have an overview of the enrichments of N, Si and P on the growth and nutrient uptake of the experimental phytoplankton communities, a combined plot has been presented in Fig. 11. The first panel (Fig. 11a) depicts the maximum growth rates in terms of different nutrient enrichments. Nitrate enrichment showed the highest growth response nearly at $65\mu\text{M}$ nitrate level with a linear increasing trend. Si induced growth response was highest at $55\mu\text{M}$ and P showed at $\approx 10\mu\text{M}$ levels. P uptake continued up to the maximum P level P (Fig. 11b). In the case of N and Si enrichment, the maximum uptake levels were observed at $\approx 65\mu\text{M}$, whereas the highest growth response was seen at $55\mu\text{M}$ for Si. This observation suggested that for Si non-saturating uptake kinetics was followed up to this level.

Nutrient removal potential of phytoplankton:

Nutrient removal rates were calculated per unit biomass (*Chla*) per day from all experiments. The maximum Si removal rate noticed in Exp I was $1.52 \mu\text{mol Chla}^{-1} \text{d}^{-1}$ at $65\mu\text{M}$ Si level. This rate showed almost 5 times a decrease at the lowest Si level. Exp-II revealed a Si removal rate of $1.22 \pm 0.29 \mu\text{mol Chla}^{-1} \text{d}^{-1}$ and this value was $1.32 \pm 0.65 \mu\text{mol Chla}^{-1} \text{d}^{-1}$ in Exp III. Si levels in both the experiments were $100\mu\text{M}$. P removal rates were 0.11 ± 0.02 and $0.15 \pm 0.02 \mu\text{mol Chla}^{-1} \text{d}^{-1}$ in Exp-IA and IB, respectively. P levels were 5 times higher in Exp-IB than Exp IA. P removal rate recorded in Exp-III was $0.086 \pm 0.02 \mu\text{mol P Chla}^{-1} \text{d}^{-1}$ under $10\mu\text{M}$ P. The same rate showed a value of $0.05 \pm 0.01 \mu\text{mol P Chla}^{-1} \text{d}^{-1}$ at $4\mu\text{M}$ P level and increased more than 3 times ($0.16 \mu\text{mol P Chla}^{-1} \text{d}^{-1}$) at the last three treatments (highest concentrations). This suggested that an enhancement in P supply by 4 times correspondent to a 3 fold increase in the P removal rate by phytoplankton. The average N removal rates from Exp-IA ($0.49 \pm 0.08 \mu\text{mol Chla}^{-1} \text{d}^{-1}$) increased almost 2.5 times ($1.22 \pm 0.22 \mu\text{mol Chla}^{-1} \text{d}^{-1}$) for 5 times increase in N supply. The maximum N removal rate derived from Exp-III was $0.84 \mu\text{mol Chla}^{-1} \text{d}^{-1}$ seen at $34\mu\text{M}$ N level and the other values didn't differ significantly. Since *Chla* synthesis is closely associated with N availability, the rate of N removal per unit *Chla* may deviate from a linear trend. We have taken the maximum N, Si and P removal rates

from the saturated concentrations and averaged to get a number that can be used for eutrophic condition. N, Si and P removal rates were 1.03 ± 0.27 , 1.35 ± 0.14 and $0.14 \pm 0.02 \mu\text{molChl}a^{-1} \text{d}^{-1}$, respectively. These revealed a ratio of 7.5:9.8:1 for N:Si:P removal rates under a nutrient saturated condition for the coastal Bay.

Discussion

Community response

The coastal waters of BoB are usually dominated by diatoms (Bandyopadhyay *et al.* 2017; Bharathi *et al.* 2018). The dominance of Fuco along with other accessory pigments (Chl c_2 , DD, DT, β -carotene) confirmed the dominance of diatom dominated microphytoplankton in the experimental communities (Exp-II and III). The coastal BoB receives a significant amount of land runoff and river discharge during the SW monsoon (>70%) and the occurrences of diatom bloom in association with increased rainfall, land runoff and Si enrichment have been reported in our earlier studies (Biswas *et al.* 2010; Shaik *et al.* 2015; Bandyopadhyay *et al.* 2017). Very recently, Bharathi and Sharma (2019) examined the phytoplankton community structure of 28 major and minor Indian estuaries and noticed that monsoon induced river discharge significantly controlled phytoplankton biomass and community composition. Therefore, our first experiment is in agreement with the earlier observations and showed that a Si enriched condition is likely to be responsible for the dominance of certain diatom species in the coastal BoB.

The occurrences of a trace amount of Zea suggested a very less quantity of cyanobacterial (pirophytoplankton) presence. Diatoms possess highly efficient nutrient storage capacity compared to cyanobacteria. Moreover, under nitrate replete conditions, diatoms usually dominate, whereas ammonia enrichment promotes cyanobacterial Growth (Berg *et al.* 2003). A significant decrease in Zea containing picophytoplankton with a concomitant increase in diatoms in response to increasing nitrate supply also supported this view. Since Si concentrations were at saturated levels, non-siliceous smaller phytoplankton like cyanobacteria (Zea containing picophytoplankton) could not probably compete with diatoms. However, pigment-based community analysis does not provide the details about species-specific changes in of community and hence microscopic analysis is needed.

During the first experiment, the phytoplankton community was mostly dominated by the chain-forming centric diatom *Chaetoceros* spp.(data is not shown here) which has been reported to uptake dissolved silicate more efficiently and at a much faster rate relative to other large diatoms like *Rhizosolenia* (Tréguer *et al.* 1991). Tantanasarit *et al.* (2013) conducted a study on *Chaetoceros calcitrans* under the nutrient replete condition and observed very high Si consumption along with N and P uptake. For this characteristic probably, *Chaetoceros* has been reported as one of the most

commonly occurring species in the coastal BoB (Bharathi *et al.* 2018). The seasonal nutrient cycle in the coastal BoB changes drastically and so the phytoplankton community structure. During an environmental impact assessment study, Shaik *et al.* (2017) noticed that in a coastal station of BoB, high phytoplankton biomass dominated by *Chaetoceros* spp. (57%) was associated with low saline Si enriched condition ($\approx 12\mu\text{M}$) during the late post-monsoon season (Dec). During the pre-monsoon (March), Si level decreased to half and led to a significant reduction in *Chaetoceros* spp. relative abundance coupled with increased pennate diatom (*Nitzschia* spp.) abundance. This observation suggested that Si replete condition promoted *Chaetoceros* spp., whereas, at low Si levels, the pennate diatom dominated. This could be due to their higher surface area to volume ratio which allows them to uptake maximum Si even at very low concentration. Burson *et al.* (2018) noticed a similar trend in a coastal phytoplankton community. This is also important to mention that not all diatoms are equally efficient in nutrient consumption and storage. Due to this fact, when nutrient levels start to exhaust with the progression of growth, only certain species benefit from their higher nutrient storage efficiency. This characteristic feature finally shapes a community.

In shallow coastal waters, the phytoplankton community structure can be tightly coupled with the N budget (Philippart *et al.* 2000). Our nitrate enrichment experiment also revealed a similar trend. Biswas *et al.* (2010) noticed that phytoplankton community structures in a diatom dominated assemblages from a Si enriched mangrove water (NE coast of BoB) were significantly correlated with N:P loading (related to rainfall pattern and tidal cycles). The species-specific response of phytoplankton to certain nutrient limitation or enrichment plays a key role in configuring the community structure (Lagus *et al.* 2004). Intracellular nutrient pool capacity for a particular nutrient can be highly variable within diatoms and that finally shapes nutrient uptake kinetics and species dominance. The increasing abundance of *Thalassiosira* spp. in response to nitrate enrichment coupled with decreased *Chaetoceros* spp. abundance indicated that the competitive efficiency of consuming nitrate under the Si and P replete conditions was higher in the former genera compared to the latter. Sarma *et al.* (2010) also noticed *Thalassiosira* abundance over *Chaetoceros* in the Godavari estuary during the postmonsoon season.

Diatoms can uptake and store a significantly higher amount of N than their requirement (Lomas & Gilbert, 2000). Li & Campbell (2017) noticed in an experimental study that a smaller sized coastal diatom (*Thalassiosira*) out competed a larger diatom with a slower growth rate. The former species also grew faster and contained enhanced protein content per cell under in response to N enrichment. Colls *et al.* (1997) noticed that *Thalassiosira* showed non-saturating uptake kinetics for nitrate at $50\mu\text{M}$ level in a natural phytoplankton assemblage from a coastal lagoon. On the

contrary, *Chaetoceros* spp. reached the saturation (Michaelis Menten type) level very quickly. This was directly related to their internal nutrient pool capacity. This observation is in good agreement with our results and explains why there was an increasing abundance of *Thalassiosira* spp. with a concomitant decrease in *Chaetoceros* at 65 μ M nitrate level. This observation suggests that the high nitrate uptake potential of this genus can provide them a competitive advantage over the others and probably, therefore, *Thalassiosira* spp. is one of the most abundant diatom genera in the coastal Bay during the SW monsoon (Bharathi *et al.* 2018). Unfortunately, we did not have any presentable microscopic data for the Si and P enrichment experiments which could have revealed more information regarding community shift.

Physiological response: Growth and nutrient removal

Diatoms are well known for 1) responding quickly to any type of nutrient pulses and 2) luxury nutrient uptake (Paasche *et al.* 1973; Tilman & Kilham, 1976; Harrison *et al.* 1989). A similar trend was observed in the present study. The maximum removal rate was noticed for Si. Interestingly, the Si removal rate at the lowest Si level was almost 5 times lower than that of the highest level Si level at 65 μ M. This indicates that upon 7 times enhancement in Si supply in this coastal water (particularly during the monsoon), phytoplankton may increase their Si removal rate by 5 times. Moreover, as mentioned earlier that the average Si levels, noticed in the estuarine waters of Ganges and Godavari (Biswas *et al.*, 2004; Muphopadhyay *et al.* 2006; Biswas *et al.* 2010; Sarma *et al.* 2010) were also \approx 60 μ M and very close to the growth saturating concentration of Si (55 μ M) observed in this experiment.

From the Chemostat experiments, three types of Si uptake and Si dependent growth patterns have been predicted for diatoms (Conway *et al.* 1976; Hildebrand & Whetherbee, 2003). A surge uptake has been observed when Si starved cells were supplied with sufficient Si. In the 2nd type, Si uptake has been said to be controlled by the external Si concentrations; in the third type, Si uptake is dependent on the rate of Si incorporation in the diatom cell wall. In the present experiment, the cells were not Si starved, but most likely to be Si limited after the exponential growth phase in the stock culture. This may lead to a linear increase in Δ Si and Si removal rate with increasing Si supply beyond the growth saturating Si level (55 μ M). After the exponential growth phase, Δ Si reached a plateau showing the difference in Si consumption during an exponential and stabilized growth phase. This excess Si uptake after the growth saturating phase can be attributed to “luxury consumption”. According to Droop (1977), the “luxury consumption” is the ratio of the cell quota for a particular nutrient under nutrient limitation and nutrient replete condition. The observed increase in the concentrations of Chla and BSi along with BSi:Chla ratios up to 65 μ M Si level suggested that

during this phase Si was probably used for cell division and growth. Whereas further Si enrichment did not show such linearity and perhaps the uptake was “luxury” at this stage. After the growth saturating Si level, the Si removal rate also stabilized. A similar trend was seen in the growth rate, Δ Si and BSi contents in response to increasing Si supply during a natural diatom bloom (Kristinasen *et al.* 2004). Further, the results also revealed that when other nutrients (P and N) are not growth-limiting, there could be a luxury uptake of the third nutrient (Si). The difference in N and P contents between Exp-IA and Exp-IB did not impact BSi formation. This suggested that BSi production was mainly controlled by Si enrichment and the rate of silica incorporation in the cell wall was independent of nitrogen supply when N is not limiting. Unlike nitrogen metabolism, which needs reductant from photosynthesis, Si metabolism can go ahead independently (Martin-Jézéquel *et al.* 2000).

Si is obligatory for diatom growth (Brzezinski & Conley, 1994) and Si starvation results in the complete cessation of cell division (Werner, 1977). Si uptake and its deposition on the cell wall do not occur evenly throughout the cell cycle but usually associated with the phase of cytokinesis and separation of the daughter cells when new siliceous valves form. Therefore, Si uptake increases just before the cell division (Sullivan, 1977; Crawford & Schmid, 1986). Diatom girdle bands and setae formations take place during the growth phase after the cell division (Rogerson *et al.* 1986). Diatoms probably cannot store Si as they do for N or P (Lomas & Gilbert, 2000; Egge & Aksnes, 1992) and the internal dissolved Si is the only pool they can use. However, Si intracellular pool can be very high compared to its saturation level.

Unlike N and P, Si has a specific feature that dissolved Si molecules polymerize when internal Si concentrations exceed 2mM. Thamatrakoln and Hildebrand (2008) conducted a study on the Si uptake rates in multiple marine diatoms and showed that initially Si uptake was non-saturating and became saturating after a certain level. This observation is comparable to our results. Further, the authors concluded that Si uptake can be directly dependent on the intracellular Si pool capacity which varies depending on the growth phase. During the high pool capacity, the non-saturating uptake kinetics can be seen. With decreasing intracellular Si pool size, the saturation occurs after a certain Si level. In our Si enrichment experiments, it was close to 50-60 μ M Si levels where the community showed a saturating uptake and hence, a further increase in Si supply did not impact growth.

Δ P values and P removal rates per unit biomass per day were tightly coupled with increasing P levels and showed a non-saturating uptake kinetic. Tilman & Kilham (1976) showed that diatoms can uptake 6-8 times higher P than required for growth. Usually, they store P as P-rich nucleic acid.

The average P removal rate noticed within the first four P treatments (usually seen in this coastal water) was $0.05\mu\text{mol Chl}a^{-1} \text{d}^{-1}$. This value tripled at the highest P treatment suggesting that in case of an increase in P loading along with N and Si, this is likely to increase P removal efficiency by three-fold. However, when Si and N levels are not sufficient, this trend may not be valid. Enhanced growth response of a coastal phytoplankton community in response to P enrichment was also reported by earlier authors (Duarte *et al.* 2000). It was noticed that under N and Si replete conditions, P deficiency can hamper phytoplankton growth and efficient utilization of those nutrients. The difference in P removal rate between Exp-IA and IB also shows that a 5-time reduction in P level can be responsible for restricted P removal. Hence, any additional supply of P in coastal waters can be efficiently removed by phytoplankton followed by a conversion of inorganic to organic P or dissolved to particulate P. ΔSi was coupled with increasing P level within the growth saturating level (up to $10\mu\text{M P}$); further, increase in ΔP was probably due to luxury consumption and therefore ΔSi values decoupled. Increased BSi contents with increasing P was mostly due to increased cell division rates and was confirmed by the nonlinearity of BSi:Chl*a* ratio with P levels. $\Delta\text{P}:\Delta\text{Si}$ ratios were well correlated with P concentrations and this was likely to be influenced by P uptake kinetics, rather than ΔSi . When Si is limiting, Si transport by diatoms can be done actively at the cost of energy and may show a correlation with P levels since P is utilized for ATP production. In the present study, Si was not limiting, and hence the diffusive Si uptake seemed to be the key process of Si transport inside the cell.

N is a vital nutrient for marine phytoplankton for synthesizing some essential cellular materials related to cell division and growth. Therefore, N loading significantly impacts phytoplankton biomass and primary production in coastal waters (Borum & Sand-Jensen, 1996). Moreover, the types of inorganic N forms supplied to phytoplankton are a key factor that controls the phytoplankton community structure (Gilbert *et al.* 2016). Nitrate was seen to be the preferred inorganic nitrogen species for diatoms, whereas cyanobacteria favored ammonia (Berg *et al.* 2003). The observed insignificant correlation between Zea and nitrate concentrations also supports this view. However, there is a considerable knowledge gap regarding our understanding of phytoplankton response to the "excess N" supply when present at saturated levels (Gilbert *et al.* 2013; Gilbert *et al.* 2016). Our study revealed that increasing N supply in the form of nitrate boosted growth rate, BSi production, protein contents, and total pigment synthesis as well as nutrient consumption in the experimental phytoplankton community. Like Si and P, diatoms can show luxury uptake of nitrate even when a system is not nitrate limited. Mackey *et al.* (2014) noticed in the Californian upwelling system that diatoms showed significantly high nitrate ($10\mu\text{M}$) consumption when nitrate was not

limiting (13-30 μ M). This study supports our observation. Interestingly, the highest N removal rate was not seen at the highest N supply, but at 34 μ M N level. Moreover, the increase in the N removal rate was not significantly different (<10%) between the treatments. This could be because N has significant linear positive impacts on Chl*a* synthesis and therefore, normalizing with Chl*a* may not yield the actual rate. In case, the magnitude of increase in N uptake and Chl*a* synthesis are almost similar, the rate may show low variability. However, N induced growth rate can be coupled only up to the growth saturating concentrations of nitrate, and after that level, the uptake was mostly luxury type.

N and carbon assimilations are two closely coupled cellular processes. For nitrogen assimilation and amino acid biosynthesis, the required reducing equivalents are procured through the Calvin cycle of photosynthesis (Hockin *et al.* 2012). At first, nitrate gets reduced to nitrite and then to ammonia and finally incorporated into amino acid and protein. And therefore, upon the supply of additional nitrate, a steady-state photosynthetic rate can be achieved. The exponential increase in Chl*a* contents confirms that the photosynthetic rate increased in response to increased nitrogen supply. The linearity between Δ N concentrations and protein contents confirmed that increasing N supply accelerated N metabolism in the presence of sufficient organic carbon. The ratios of Δ Si: Δ N also suggested that under N enriched condition, the relative uptake of N was higher than Si and hence a decreasing trend was noticed with increasing N addition. In a recent study by Alipanah *et al.* (2015), it was noticed that when N starved diatom cells were supplemented with N, the gene expressions responsible for photosynthesis, carbohydrate metabolism, protein and chlorophyll synthesis enhanced. In the present study, increased protein content in response to enhanced nitrate addition also indicated a similar trend. In the Exp -IA, the inverse correlation between Δ N and Si levels explains higher Si uptake rates over N in response to increasing Si addition. However, unlike Si, the growth saturating and the highest N uptake levels occurred at \approx 65 μ M. The high requirement of N in cellular metabolism is likely to be responsible for such a trend.

HPLC pigment analysis clearly showed that an increase in N supply increased TP, chlorophylls (Chl*a* and Chl*c*₂) and other accessory pigment contents. Carotenoids like Fuco, Zea and DD+DT also increased with an increasing nitrogen source, but were not statistically significant, because unlike chlorophylls these pigments do not contain nitrogen in their molecular structures (Jeffrey and Vesk, 1997). Hindrance in chlorophyll synthesis in the absence of sufficient N source in marine diatoms has been reported long back (Harvey, 1958). During the present study, the observed enhancement in Chl*a* and Chl*c*₂ contents in response to N enrichment also supports this view. Decreased value of BSi:Chl*a* ratios were probably due to the higher magnitude of enhancement in

Chla relative to BSi in response to N enrichment. In the P enrichment experiment, an initial exponential increase in Chla, β -carotene and Fuco were mostly correlated to general growth enhancement. This trend was not seen after 4.4 μ M P addition and suggested that probably after this level P wasn't used in pigment synthesis related processes.

Conclusions

The coastal Bay of Bengal is likely to turn more eutrophic with increasing population density and agricultural activities. Further, the future increase in the number and intensity of the tropical cyclones in this Bay may potentially impact its nutrient stoichiometry. The present experiment clearly showed that nutrient removal efficiencies of coastal phytoplankton are significantly high in this region and justifies their role as a filter for eutrophicated coastal waters. In case of any additional nutrient pulse in this coastal water, diatoms will be the major group to respond immediately and may consume nutrients without following the Redfield Ratio. If N is added to this coastal water in the form of nitrate under Si replete condition, diatoms will be the winners and may efficiently suppress cyanobacterial growth. Reduction in Si supply and an increase in ammonia may reverse the situation. Any such change in the phytoplankton community in response to nutrient stoichiometry will have immediate impacts on the food chain. Considering the future scenario, this is likely that aggressive nutrient consumption by coastal phytoplankton will also alter the elemental stoichiometry of organic matter and can be further transmitted to higher trophic levels. Moreover, organic matter sinking to the sediment will also have some impacts on the benthic community. However, the lack of microscopic analyses from Si and P enrichment experiments restricts to provide some important information on phytoplankton species-specific response. More experimental studies are essential to predict future changes in the phytoplankton community and its consequences on coastal water health and ecosystem services. Finally, coastal waters are also experiencing warming and low pH condition, which may exert further impacts on the phytoplankton community. Therefore, a multi-stressor approach should be considered for any future study.

Acknowledgments

The first author is thankful to the Council of Scientific and Industrial Research (CSIR) for financial support. The kind support and cooperation provided by the Director, CSIR-NIO, and Scientist-In-Charge, Regional Centre, NIO, Visakhapatnam is also gratefully acknowledged. All colleagues from Regional Centre, Visakhapatnam are gratefully acknowledged for their active cooperation and help during the study. (NIO contribution number for this publication is XXX).

Author contribution

D. Bandyopadhyay: experimenting, all laboratory analyses, preparing the figures and drafting the manuscript; H. Biswas: original idea of the experiments, experimenting, editing and finalizing the manuscript.

References

- Alipanah, L., Rohloff, J., Winge, P., Bones, A.M. and Brembu, T. (2015). Whole-cell response to nitrogen deprivation in the diatom *Phaeodactylum tricornutum*. *Journal of Experimental Botany*, **66**:6281-6296.
- Amo, Y.D. & Brzezinski, M.A. (1999). The chemical form of dissolved Si taken up by marine diatoms. *Journal of Phycology*, **35**:1162-1170.
- Bandyopadhyay, D., Biswas, H. and Sarma, V.V.S.S. (2017). Impacts of SW monsoon on phytoplankton community structure along the western coastal BOB: an HPLC approach. *Estuaries and Coasts*, **40**:1066-1081.
- Balaguru, K., Taraphdar, S., Leung, L. R., & Foltz, G. R. (2014). Increase in the intensity of postmonsoon Bay of Bengal tropical cyclones. *Geophysical Research Letters*, **41**: 3594-3601.
- Berg, G. M., Balode, M., Purina, I., Bekere, S., Béchemin, C., & Maestrini, S. Y. (2003). Plankton community composition in relation to availability and uptake of oxidized and reduced nitrogen. *Aquatic microbial ecology*, **30**: 263-274.
- Bharathi, M.D., Sarma, V.V.S.S., Ramaneswari, K. and Venkataramana, V. (2018). Influence of river discharge on abundance and composition of phytoplankton in the western coastal Bay of Bengal during peak discharge period. *Marine pollution bulletin*, **133**:671-683.
- Biswas, H., Mukhopadhyay, S. K., De, T. K., Sen, S., & Jana, T. K. (2004). Biogenic controls on the air—water carbon dioxide exchange in the Sundarban mangrove environment, northeast coast of Bay of Bengal, India. *Limnology and Oceanography*, **49**: 95-101.
- Biswas, H., Shaik, A. U. R., Bandyopadhyay, D., and Chowdhury, N. (2017). CO₂ induced growth response in a diatom dominated phytoplankton community from SW Bay of Bengal coastal water. *Estuarine and Continental Shelf Research*. **198**: 29-42.
- Biswas, H., Dey, M., Ganguly, D., De, T.K., Ghosh, S. and Jana, T.K. (2010). Comparative analysis of phytoplankton composition and abundance over a two-decade period at the land—ocean boundary of a tropical mangrove ecosystem. *Estuaries and Coasts*, **33**:384-394.
- Boesch, D. F. (2019). Barriers and Bridges in Abating Coastal Eutrophication. *Frontiers in Marine Science*, **6**, 123.
- Borum, J., & Sand-Jensen, K. (1997). Is total primary production in shallow coastal marine waters stimulated by nitrogen loading?. *Oceanographic Literature Review*, **1**: 40-41.

- Brembu, T., Mühlroth, A., Alipanah, L., & Bones, A. M. (2017). The effects of phosphorus limitation on carbon metabolism in diatoms. *Philosophical Transactions of the Royal Society B: Biological Sciences*, **372**:20160406.
- Brzezinski, M. A. (1985). The Si: C: N ratio of marine diatoms: Interspecific variability and the effect of some environmental variables, *Journal of Phycology*, **21**:347-357
- Brzezinski, M.A. & Conley, D.J. (1994). Silicon deposition during the cell cycle of *Thalassiosira weissflogii* (Bacillariophyceae) determined using dual rhodamine and propidium iodide. *Journal of Phycology*, **30**:45-55.
- Burson, A., Stomp, M., Akil, L., Brussaard, C.P. and Huisman, J. (2016). Unbalanced reduction of nutrient loads has created an offshore gradient from phosphorus to nitrogen limitation in the North Sea. *Limnology and Oceanography*, **61**:869-888.
- Burson, A., Stomp, M., Greenwell, E., Grosse, J., & Huisman, J. (2018). Competition for nutrients and light: testing advances in resource competition with a natural phytoplankton community. *Ecology*, **99**: 1108-1118.
- Chen, N., Wu, Y., Wu, J., Yan, X. and Hong, H. (2014). Natural and human influences on dissolved silica export from watershed to coast in Southeast China. *Journal of Geophysical Research: Biogeosciences*, **119**:95-109.
- Cira, E.K., Paerl, H.W. and Wetz, M.S. (2016). Effects of nitrogen availability and form on phytoplankton growth in a eutrophied estuary (Neuse River Estuary, NC, USA). *PloS one*, **11**:e0160663.
- Conley, D.J. & Malone, T.C. (1992). Annual cycle of dissolved silicate in Chesapeake Bay: implications for the production and fate of phytoplankton biomass. *Marine ecology progress series. Oldendorf*, **81**:121-128.
- Conway, H.L., Harrison, P.J. and Davis, C.O. 1976. Marine diatoms grown in chemostats under silicate or ammonium limitation. II. Transient response of *Skeletonemacostatum* to a single addition of the limiting nutrient. *Marine Biology*, **35**:187-199.
- Crawford, R. M. & Schmid, A. M. (1986). Ultrastructure of silica deposition in diatoms. In *Biom mineralization in lower plants and animals* (Leadbeater, B. S. C. & Riding, R., editors), 291–314. Clarendon Press, Oxford.
- Davidson, K. & Gurney, W.S.C. (1999). An investigation of non steady state algal growth II. Mathematical modelling of co-nutrient limited algal growth. *Journal of Plankton Research*. **21**:839–858.
- Donald, D. B., Bogard, M. J., Finlay, K., Bunting, L., & Leavitt, P. R. (2013). Phytoplankton-specific response to enrichment of phosphorus-rich surface waters with ammonium, nitrate, and urea. *PloS one*, **8**: e53277.
- Droop, M. R. (1974). The nutrient status of algal cells in continuous culture. *Journal of the Marine Biological Association of the United Kingdom*, **54**:825-855.

- Duarte, C.M., Agusti, S. and Agawin, N.S. (2000). Response of a Mediterranean phytoplankton community to increased nutrient inputs: a mesocosm experiment. *Marine Ecology Progress Series*, **195**:61-70.
- Egge, J. K. & Aksnes, D. L. (1992). Silicate as regulating nutrient in phytoplankton competition. *Marine ecology progress series. Oldendorf*, **83**:281-289.
- Gao, C. & Zhang, T. (2010). Eutrophication in a Chinese context: understanding various physical and socio-economic aspects. *Ambio*, **39**: 385-393.
- Garnier, J., Beusen, A., Thieu, V., Billen, G. and Bouwman, L. (2010). N: P: Si nutrient export ratios and ecological consequences in coastal seas evaluated by the ICEP approach. *Global Biogeochemical Cycles*, **24**:GB0A05, 1-12.
- Martiny, A. C., Pham, C. T., Primeau, F. W., Vrugt, J. A., Moore, J. K., Levin, S. A., & Lomas, M. W. (2013). Strong latitudinal patterns in the elemental ratios of marine plankton and organic matter. *Nature Geoscience*, **6**: 279-283.
- Girishkumar, M. S., Thangaprakash, V. P., Udaya Bhaskar, T. V. S., Suprit, K., Sureshkumar, N., Baliarsingh, S. K., J. Jofia, Vimlesh Pant, S. Vishnu, G. George, K. R. Abhilash, S. Shivaprasad, Abhilash, K. R. (2019). Quantifying tropical cyclone's effect on the biogeochemical processes using profiling float observations in the Bay of Bengal. *Journal of Geophysical Research: Oceans*, **124**: 1945-1963.
- Glibert, P. M., Wilkerson, F. P., Dugdale, R. C., Raven, J. A., Dupont, C. L., Leavitt, P. R., & Kana, T. M. (2016). Pluses and minuses of ammonium and nitrate uptake and assimilation by phytoplankton and implications for productivity and community composition, with emphasis on nitrogen-enriched conditions. *Limnology and Oceanography*, **61**: 165-197.
- Glibert, P.M., Maranger, R., Sobota, D.J. and Bouwman, L. (2014). The Haber Bosch–harmful algal bloom (HB–HAB) link. *Environmental Research Letters*, **9**:105001.
- Harrison, P. J., Parslow, J. S., & Conway, H. L. (1989). Determination of nutrient uptake kinetic parameters: a comparison of methods. *Marine Ecology Progress Series*: **52**: 301-312.
- Harvey, H.W., 1953. Synthesis of organic nitrogen and chlorophyll by *Nitzschia closterium*. *Journal of the Marine Biological Association of the United Kingdom*, **31**:477-487.
- Hildebrand, M. & Wetherbee, R. (2003). Components and control of silicification in diatoms. In *Silicon Biomineralization*. 11-57. Springer, Berlin, Heidelberg.
- Hockin, N. L., Mock, T., Mulholland, F., Kopriva, S., & Malin, G. (2012). The response of diatom central carbon metabolism to nitrogen starvation is different from that of green algae and higher plants. *Plant Physiology*, **158**:299-312.
- Jeffrey, S. W. & M, Vesk. (1997). Introduction to marine phytoplankton and their pigment signature, In *Plankton pigment in oceanography* (Jeffrey, S. W.; Mantoura, R. F. C., Wright, S. W., editors), 37–84. UNESCO Publishing.

- Karthikeyan, P., Manimaran, K., Sampathkumar, P. and Rameshkumar, L. (2013). Growth and nutrient removal properties of the diatoms, *Chaetoceros curvisetus* and *C. simplex* under different nitrogen sources. *Applied Water Science*, **3**: 49-55.
- Kristiansen, S., Farbrot, T. and Naustvoll, L.J. (2000). Production of biogenic silica by spring diatoms. *Limnology and Oceanography*, **45**: 472-478.
- Lagus, A., Suomela, J., Weithoff, G., Heikkilä, K., Helminen, H., & Sipura, J. (2004). Species-specific differences in phytoplankton responses to N and P enrichments and the N: P ratio in the Archipelago Sea, northern Baltic Sea. *Journal of Plankton Research*, **26**: 779-798.
- Laruelle, G.G., Roubex, V., Sferratore, A., Brodherr, B., Ciuffa, D., Conley, D.J., Dürr, H.H., Garnier, J., Lancelot, C., Le Thi Phuong, Q. and Meunier, J.D. (2009). Anthropogenic perturbations of the silicon cycle at the global scale: Key role of the land-ocean transition. *Global biogeochemical cycles*, **23**:GB4031: 1-17.
- Li, G., & Campbell, D. A. (2017). Interactive effects of nitrogen and light on growth rates and RUBISCO content of small and large centric diatoms. *Photosynthesis research*, **131**:93-103.
- Lomas M.W. & Gilbert P.M. (2000). Comparison of nitrate uptake, storage, and reduction in marine diatoms and flagellates. *Journal of Phycology*, **36**: 903-913.
- Mackey, K. R., Chien, C. T., & Paytan, A. (2014). Microbial and biogeochemical responses to projected future nitrate enrichment in the California upwelling system. *Frontiers in microbiology*, **5**: 632.
- Mukhopadhyay, S. K., Biswas, H. D. T. K., De, T. K., & Jana, T. K. (2006). Fluxes of nutrients from the tropical River Hooghly at the land–ocean boundary of Sundarbans, NE Coast of Bay of Bengal, India. *Journal of Marine Systems*, **62(1-2)**: 9-21.
- Redfield, A.C. (1958). The biological control of chemical factors in the environment. *American scientist*, **46**: 230A-221.
- Rogerson, A., DeFreitas, A. S. W. & McInnes, A.G. (1986). Growth rate and ultra structure of siliceous setae of *Chaetoceros gracilis* (Bacillariophyceae). *Journal of Phycology*, **22**: 56-62.
- Sarma, V. V. S. S., Prasad, V. R., Kumar, B. S. K., Rajeev, K., Devi, B. M. M., Reddy, N. P. C., ... & Kumar, M. D. (2010). Intra-annual variability in nutrients in the Godavari estuary, India. *Continental Shelf Research*, **30(19)**: 2005-2014.
- Sattar, M. A., Kroeze, C., & Strokal, M. (2014). The increasing impact of food production on nutrient export by rivers to the Bay of Bengal 1970–2050. *Marine pollution bulletin*, **80**:168-178.
- Schelske, C.L., Stoermer, E.F., Conley, D.J., Robbins, J.A. and Glover, R.M. (1983). Early eutrophication in the lower Great Lakes. *Science*, **222**:320-322.
- Shaik, A. U. R., Biswas, H., Reddy, N. P. C., Rao, V. S., Bharathi, M. D., & Subbaiah, C. V. (2015). Time series monitoring of water quality and microalgal diversity in a tropical bay under intense anthropogenic interference (SW coast of the Bay of Bengal, India). *Environmental impact assessment review*, **55**: 169-181.

- Smayda, T.J. (1990). Novel and nuisance phytoplankton blooms in the sea: evidence for a global epidemic. In: *Toxic Marine Phytoplankton* (Graneli, *et al.* editors), 29–40. Elsevier, New York.
- Strickland, J. D. & Parsons, T. R. (1972). A practical handbook of seawater analysis. Fisheries Research Board of Canada, Ottawa, Canada.
- Sullivan, C.W., 1977. Diatom mineralization of silicic acid. II. Regulation of Si(OH)₄ transporter rates during the cell cycle of *Navicula pelliculosa*. *Journal of Phycology*, **13**: 86-91.
- Tilman, D., & Kilham, S. S. (1976). Phosphate and silicate growth and uptake kinetics of the diatoms *Asterionella Formosa* and *Cyclotella meneghiniana* in batch and semicontinuous culture. *Journal of Phycology*, **12**: 375-383.
- Tréguer, P. & Van Bennekom, A. J. (1991). The annual production of biogenic silica in the Antarctic Ocean. *Marine Chemistry*, **35**: 477-487.
- Turner, R.E., Rabalais, N.N. and Justic, D. (2006). Predicting summer hypoxia in the northern Gulf of Mexico: Riverine N, P, and Si loading. *Marine Pollution Bulletin*, **52**:139-148.
- Tyrrell, T. (1999). The relative influences of nitrogen and phosphorus on oceanic primary production. *Nature*, **400**:525-531.
- Van Heukelem, L. and Thomas, C. S. (2001). Computer-assisted high-performance liquid chromatography method development with applications to the isolation and analysis of phytoplankton pigments. *Journal of Chromatography A*, **910**:31-49.
- Vidussi, F., Claustre, H., Manca, B. B., Luchetta, A., & Marty, J. C. (2001). Phytoplankton pigment distribution in relation to upper thermocline circulation in the eastern Mediterranean Sea during winter. *Journal of Geophysical Research: Oceans*, **106**: 19939-19956.
- Werner, D. (1977). Silicate metabolism. *The biology of diatoms*, **13**:111-149.
- Yool, A. & Tyrrell, T. (2003). Role of diatoms in regulating the ocean's silicon cycle. *Global Biogeochemical Cycles*, **17**:1-14.
- Zhou, M. J., Shen, Z. L. and Yu, R. C. (2008). Responses of a coastal phytoplankton community to increased nutrient input from the Changjiang (Yangtze) River. *Continental Shelf Research*, **28**:1483-1489.

Figure legends

Figure 1: Map showing the station location along the SW coast of Bay of Bengal.

Figure 2: Schematic representation of the experimental design. The green box represents the pre-culture phase. The first experiment (Exp-I) [light yellow box] was conducted in the presence of preset N and P supply with variable Si concentrations. In the first part of this experiment (Exp-IA), the concentrations of N and P were 5 times higher than the second part (Exp-IB). The light peach-colored box represents the second experiment (Exp-II). The impacts of variable P addition under preset N and Si supply were studied in this experiment. The light blue box represents the third part of this experiment (Exp-III) which addressed the effects of increasing N supply on phytoplankton growth and community under constant Si and P levels.

Figure 3: a) The concentrations of Chl_a; b) Chl_a based growth rate ($\mu_{\text{Chl}_a} \text{ d}^{-1}$); c) the concentrations of BSi; d) the ratios of BSi:Chl_a; e) the concentrations of net Si uptake (ΔSi); f) the concentration of net N uptake (ΔN) and g) net P uptake (ΔP); h) the ratios of $\Delta\text{Si}:\Delta\text{N}$; i) the ratios of $\Delta\text{P}:\Delta\text{N}$; j) the ratios of $\Delta\text{Si}:\Delta\text{P}$ with increasing Si supply under stable P (20 μM) and N (100 μM) levels in Exp-IA.

Figure 4: a) The concentrations of Chl_a; b) Chl_a based growth rate ($\mu_{\text{Chl}_a} \text{ d}^{-1}$); c) the concentrations of BSi; d) the ratios of BSi:Chl_a; e) net consumption of silicate (ΔSi); f) net consumption of nitrate (ΔN); g) net consumption of phosphate (ΔP); h) the ratios of $\Delta\text{Si}:\Delta\text{N}$; i) the ratios of $\Delta\text{P}:\Delta\text{N}$; j) the ratios of $\Delta\text{Si}:\Delta\text{P}$ with increasing Si concentrations under constant P (4 μM) and N (20 μM) levels during Exp-IB.

Figure 5: The trends of ΔSi with increasing Si supply a) up to 200 μM Si level and b) 65 μM Si level under 100 μM and 20 μM nitrate concentrations; the trends of BSi production with increasing Si supply c) up to 200 μM and d) 65 μM Si levels in the presence of 100 μM and 20 μM nitrate; Chl_a contents with increasing Si supply e) up to 200 μM Si and f) 65 μM Si levels in the presence of 100 and 20 μM nitrate; the ratios of BSi:Chl_a with increasing Si supply g) up to 200 μM and h) 65 μM Si level under 100 μM and 20 μM nitrate addition during Exp-IA and IB.

Figure 6: a) The concentrations of Chl_a; b) Chl_a based growth rate ($\mu_{\text{Chl}_a} \text{ d}^{-1}$); c) the concentrations of BSi; d) the ratios of BSi:Chl_a; e) net uptake of phosphate (ΔP); net uptake of silicate (ΔSi) up to f) 10 μM P level; g) net uptake of Si (up to 20 10 μM P addition); h) the ratios of $\Delta\text{P}:\Delta\text{Si}$ with increasing phosphate addition in Exp-II.

Figure 7: The concentrations of a) total pigment (TP); b) fucoxanthin; c) Chl_{c2}; d) diatoxanthin+diadinoxanthin; e) β -carotene; f) zeaxanthin detected in the HPLC analysis from Exp-II. The relative % of g) microphytoplankton (represents diatom) and h) picophytoplankton (mostly cyanobacteria) calculated based on the diagnostic pigment concentrations detected in HPLC pigment analysis.

Figure 8: The concentrations of a) Chl_a; b) Chl_a based growth rate ($\mu_{\text{Chl}_a} \text{d}^{-1}$); the concentration of total protein c); BSi d); the ratios of BSi:Chl_a e); net depletion (Δ) of nitrate (N) f); phosphate (P) g) and silicate (Si) h); the ratios of $\Delta\text{N}:\Delta\text{Si}$ i) and $\Delta\text{P}:\Delta\text{Si}$ j) with increasing nitrate supply during Exp-III (values = average \pm SD; n =2).

Figure 9: The concentrations of a) total pigment (TP); b) fucoxanthin; c) Chl_{c2}; d) diatoxanthin+diadinoxanthin; e) β -carotene; f) zeaxanthin detected in the HPLC analysis of the pigment extracts of Exp-III. The relative % of g) microphytoplankton (represents diatom) and h) picophytoplankton (mostly cyanobacteria) calculated based on the diagnostic pigment concentrations detected in HPLC pigment analysis (values = average \pm SD; n =2).

Figure 10: The relative abundance of different diatom species from the Exp-III under different nitrate addition. a) The community composition of the initial phytoplankton stock; the community compositions at the b) 14 μM ; c) 24 μM ; d) 34 μM and e) 64 μM nitrate levels.

Figure 11: Growth and nutrient uptake rates (Δ) from all experiments. The first panel represents (a) the maximum growth rates for all three nutrients up to the growth saturating nutrient concentrations. The second panel represents (b) the luxury uptake for all nutrients after the growth saturating phase before reaching the plateau. Three different color codes have been used to denote P (red), N (green) and Si (blue).

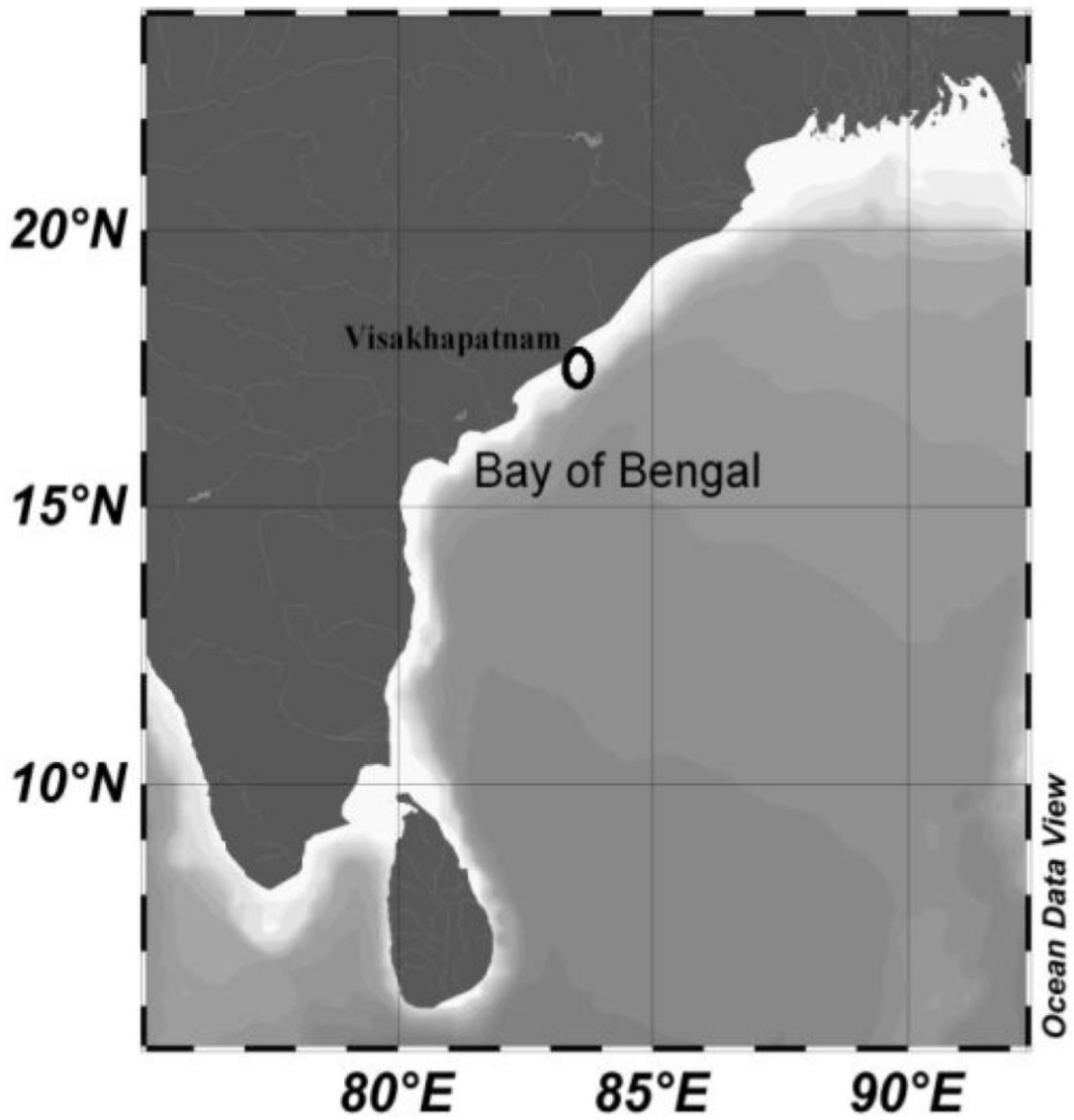


Figure 1: Map showing the station location along the SW coast of Bay of Bengal.

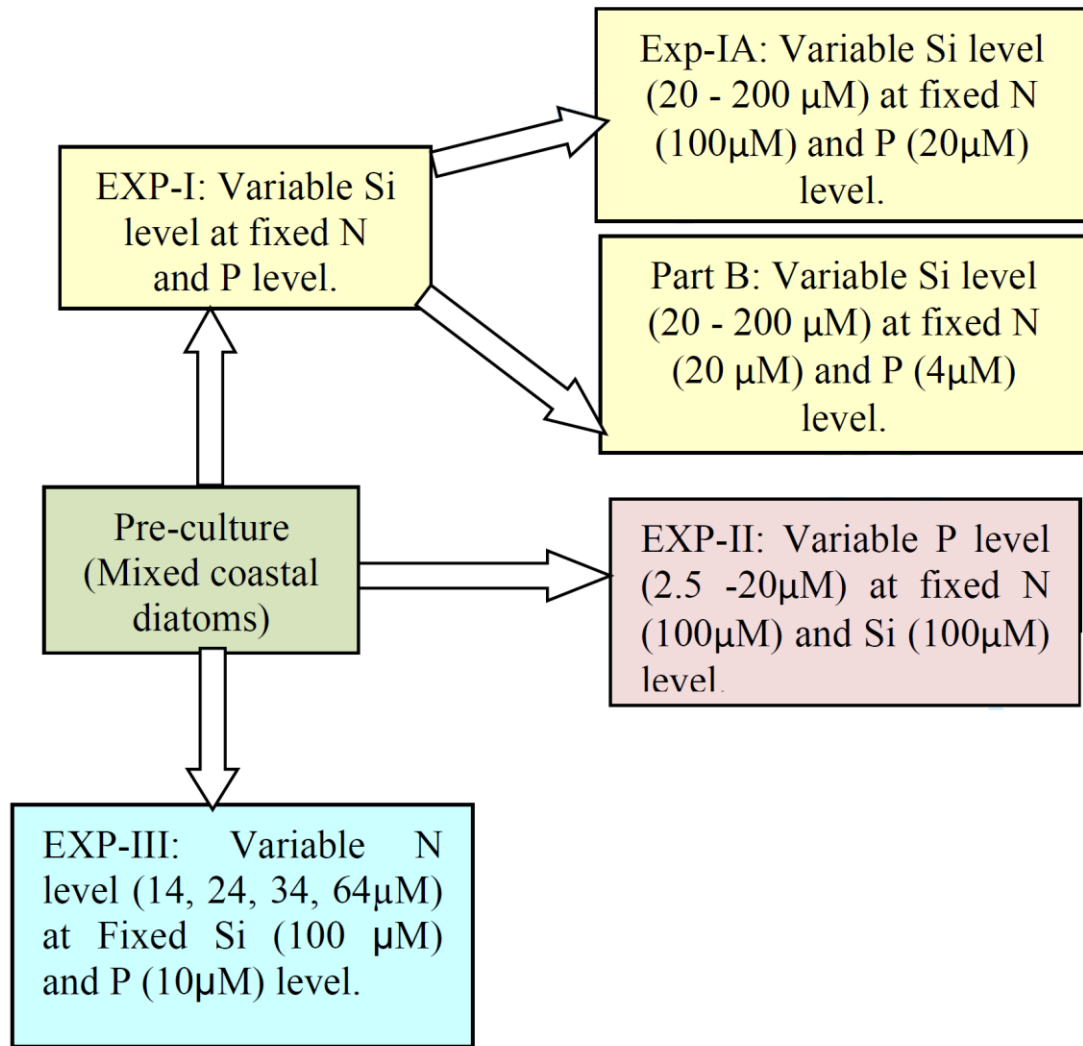


Figure 2: Schematic representation of the experimental design. The green box represents the pre-culture phase. The first experiment (Exp-I) [light yellow box] was conducted in the presence of preset N and P supply with variable Si concentrations. In the first part of this experiment (Exp-IA), the concentrations of N and P were 5 times higher than the second part (Exp-IB). The light peach-colored box represents the second experiment (Exp-II). The impacts of variable P addition under preset N and Si supply were studied in this experiment. The light blue box represents the third part of this experiment (Exp -III) which addressed the effects of increasing N supply on phytoplankton growth and community under constant Si and P levels.

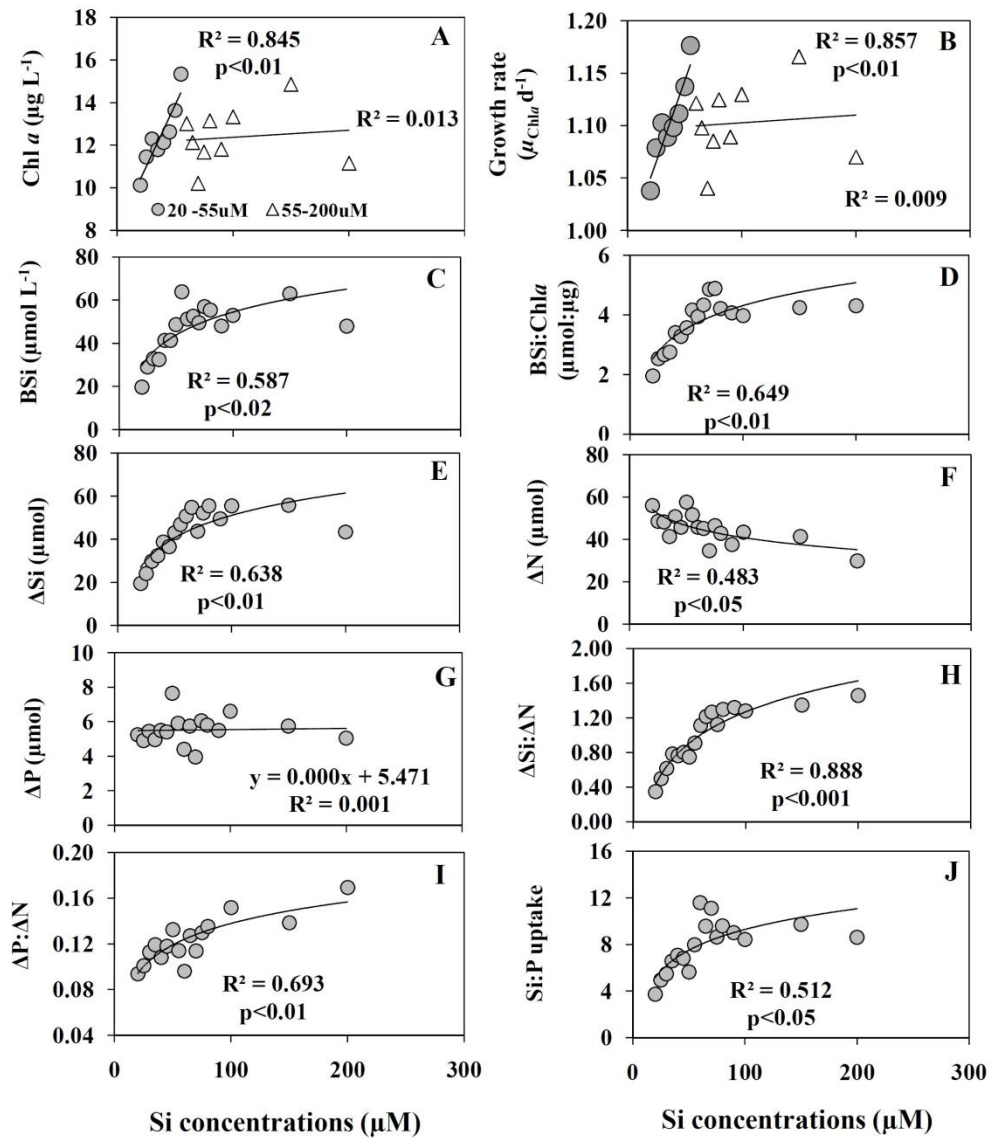


Figure 3: a) The concentrations of Chl*a*; b) Chl*a* based growth rate ($\mu_{\text{Chl}a} \text{ d}^{-1}$); c) the concentrations of BSi; d) the ratios of BSi:Chl*a*; e) the concentrations of net Si uptake (ΔSi); f) the concentration of net N uptake (ΔN) and g) net P uptake (ΔP); h) the ratios of $\Delta\text{Si}:\Delta\text{N}$; i) the ratios of $\Delta\text{P}:\Delta\text{N}$; j) the ratios of $\Delta\text{Si}:\Delta\text{P}$ with increasing Si supply under stable P (20 μM) and N (100 μM) levels in Exp-IA.

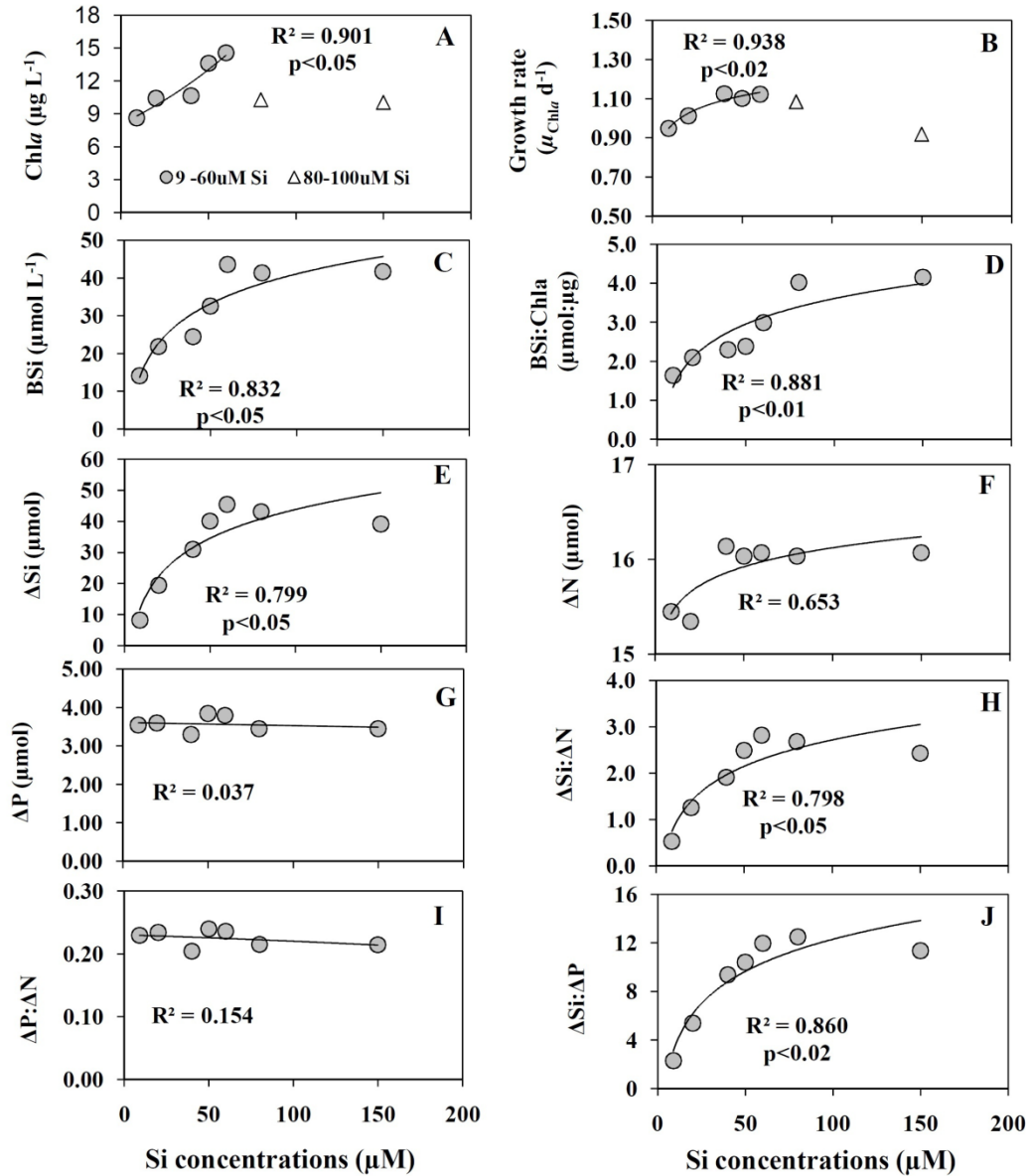


Figure 4: a) The concentrations of Chl a ; b) Chl a based growth rate ($\mu_{\text{Chl}a} \text{d}^{-1}$); c) the concentrations of BSi; d) the ratios of BSi:Chl a ; e) net consumption of silicate (ΔSi); f) net consumption of nitrate (ΔN); g) net consumption of phosphate (ΔP); h) the ratios of $\Delta\text{Si}:\Delta\text{N}$; i) the ratios of $\Delta\text{P}:\Delta\text{N}$; j) the ratios of $\Delta\text{Si}:\Delta\text{P}$ with increasing Si concentrations under constant P ($4\mu\text{M}$) and N ($20\mu\text{M}$) levels during Exp-IB.

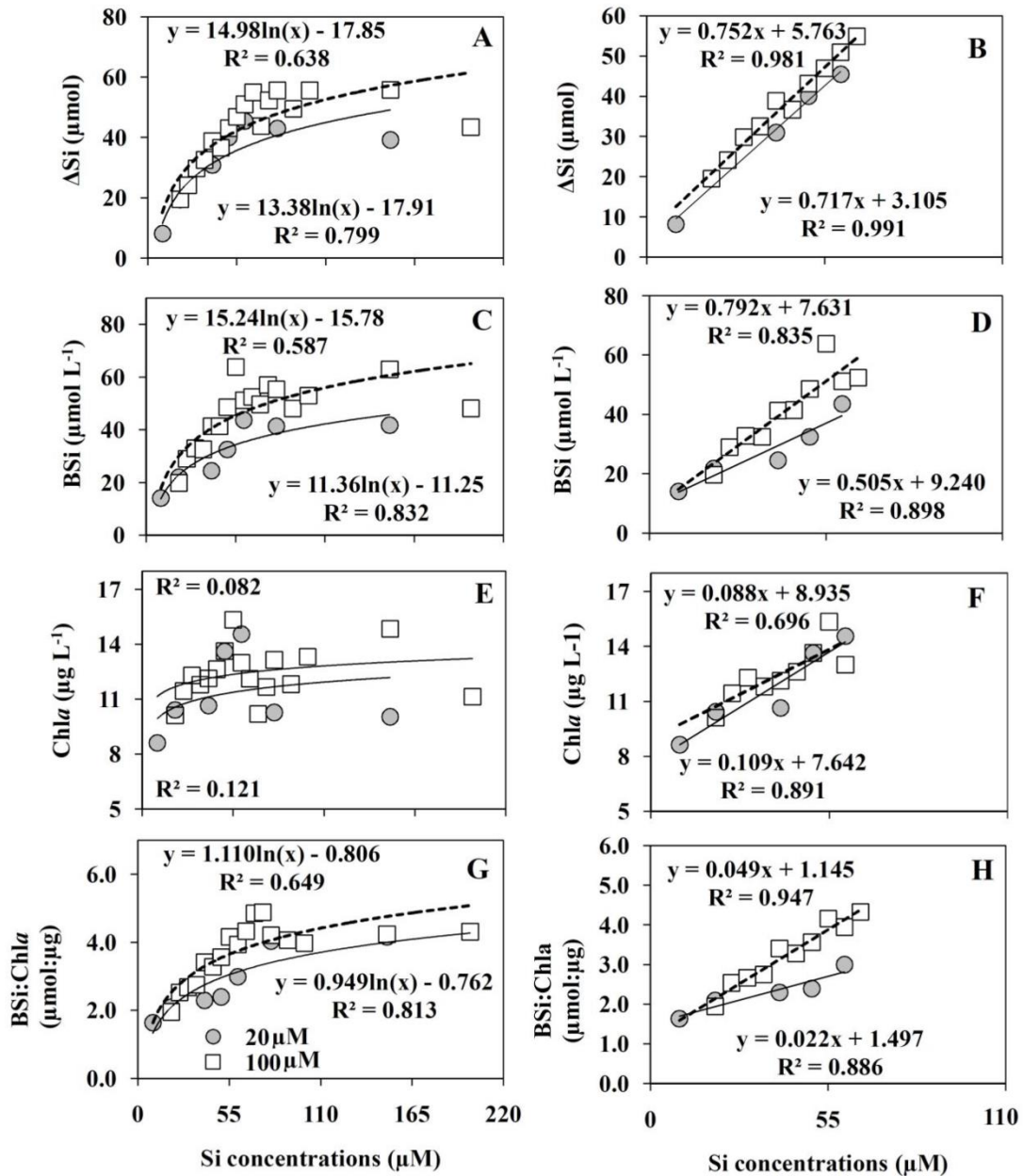


Figure 5: The trends of ΔSi with increasing Si supply a) up to 200 μM Si level and b) 65 μM Si level under 100 μM and 20 μM nitrate concentrations; the trends of BSi production with increasing Si supply c) up to 200 μM and d) 65 μM Si levels in the presence of 100 μM and 20 μM nitrate; Chl *a* contents in relation to increasing Si supply e) up to 200 μM Si and f) 65 μM Si levels in the presence of 100 and 20 μM nitrate; the ratios of BSi:Chl *a* in relation to increasing Si supply g) up to 200 μM and h) 65 μM Si level under 100 μM and 20 μM nitrate addition during Exp-IA and IB.

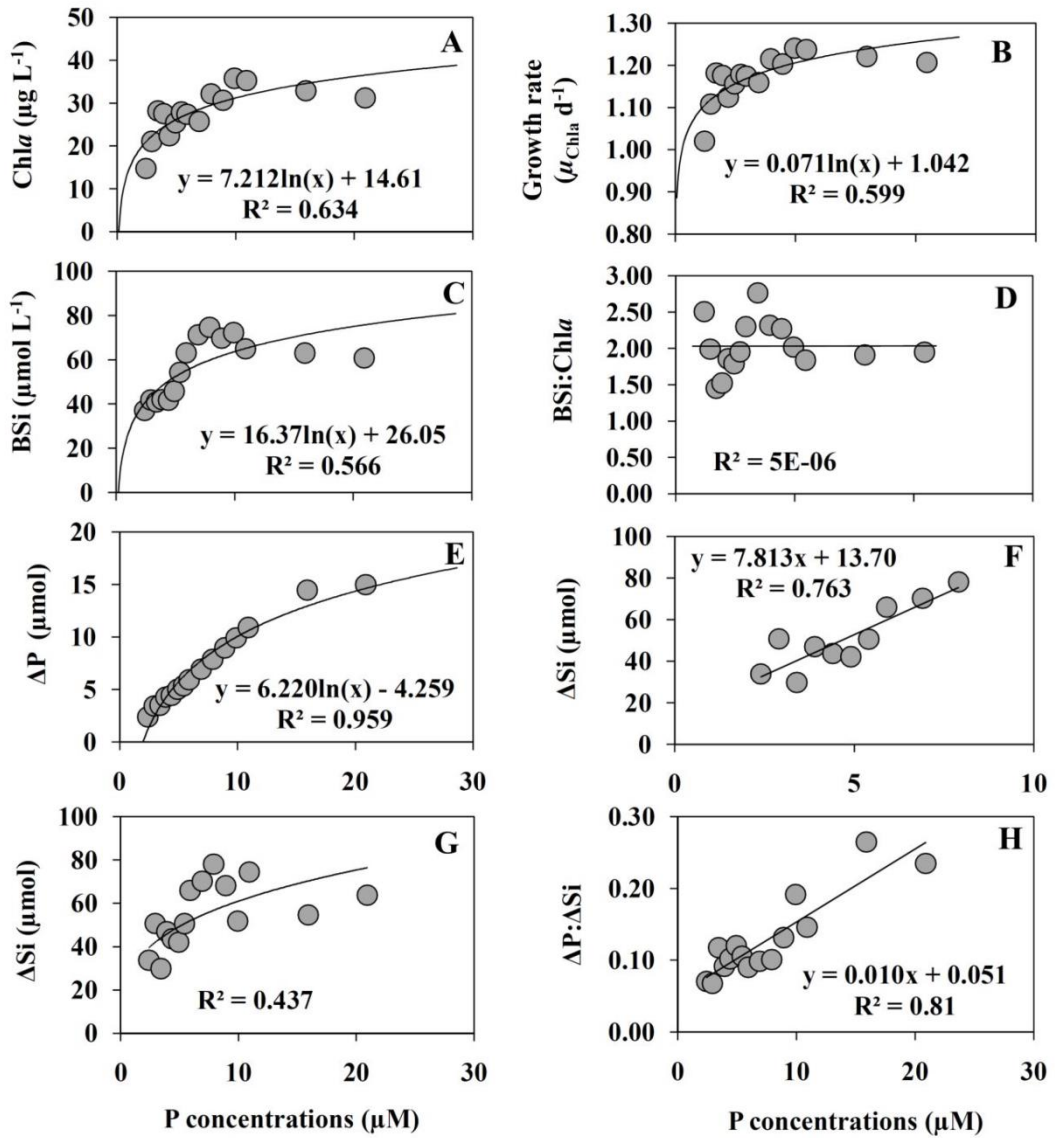


Figure 6: a) The concentrations of Chl a ; b) Chl a based growth rate ($\mu_{\text{Chl}a} \text{d}^{-1}$); c) the concentrations of BSi; d) the ratios of BSi:Chl a ; e) net uptake of phosphate (ΔP); net uptake of silicate (ΔSi) up to f) 10 μM P level; g) net uptake of Si (up to 20 10 μM P addition); h) the ratios of $\Delta\text{P}:\Delta\text{Si}$ with increasing phosphate addition in Exp-II.

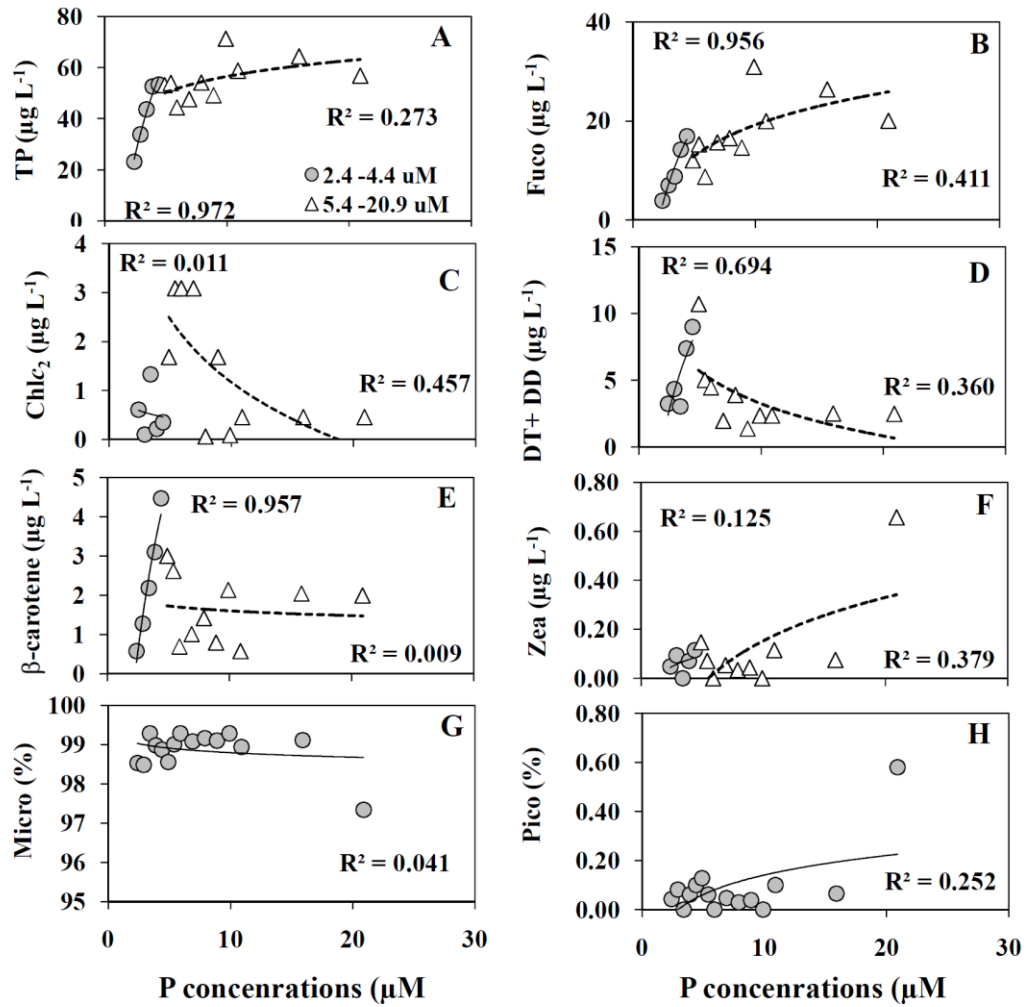


Figure 7: The concentrations of a) total pigment (TP); b) fucoxanthin; c) Chlc₂; d) diatoxanthin+diadinoxanthin; e) β -carotene; f) zeaxanthin detected in the HPLC analysis from Exp-II. The relative % of g) microphytoplankton (represents diatom) and h) picophytoplankton (mostly cynaobacteria) calculated based on the diagnostic pigment concentrations detected in HPLC pigment analysis.

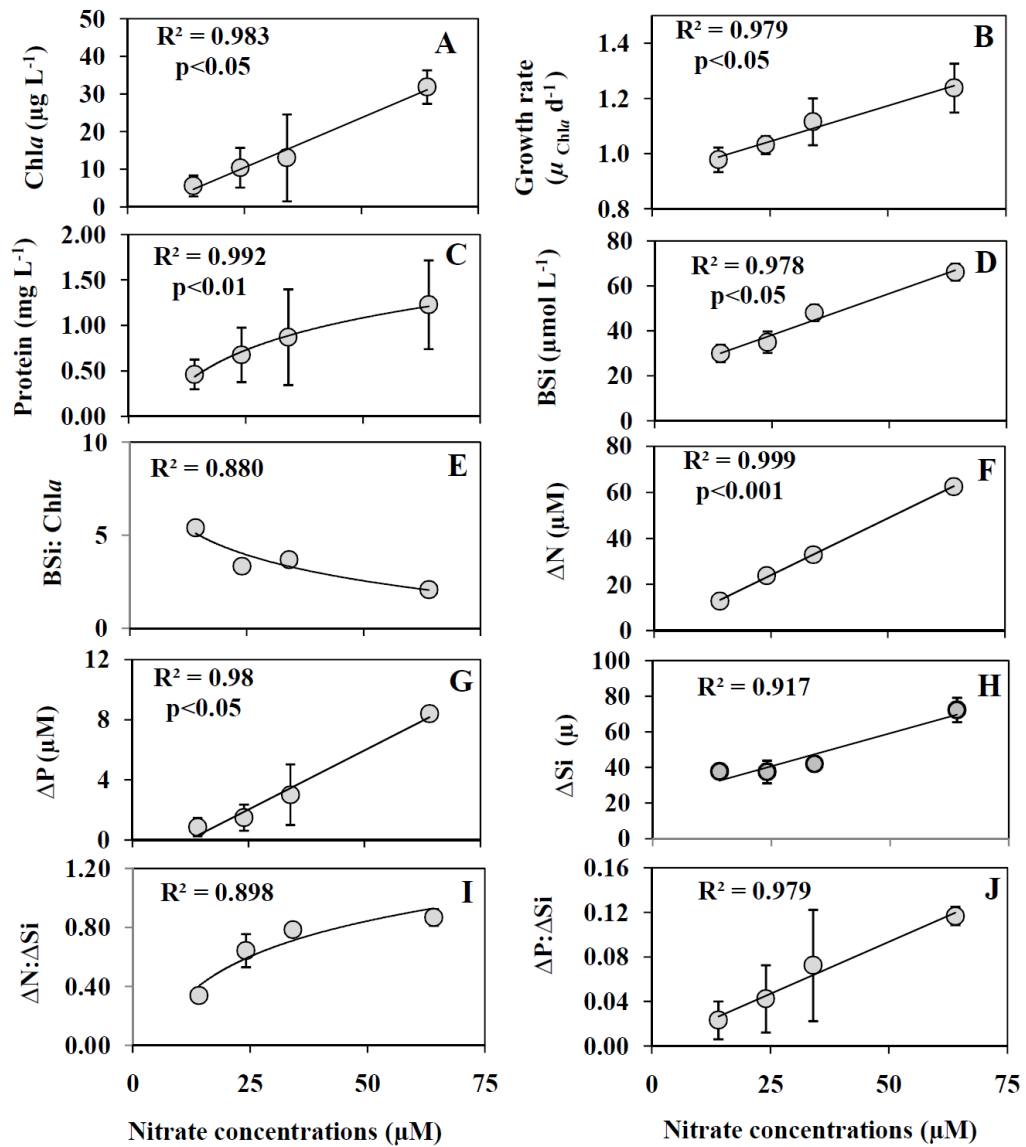


Figure 8: The concentrations of a) Chl a ; b) Chl a based growth rate ($\mu_{\text{Chl}a} \text{d}^{-1}$); the concentration of c) total protein; d) BSi; e) the ratios of BSi:Chl a ; net depletion (Δ) of f) nitrate (N); g) phosphate (P) and h) silicate (Si); the ratios of i) $\Delta\text{N}:\Delta\text{Si}$ and j) $\Delta\text{P}:\Delta\text{Si}$ in response to increasing nitrate supply during Exp-III (values = average \pm SD; n =2).

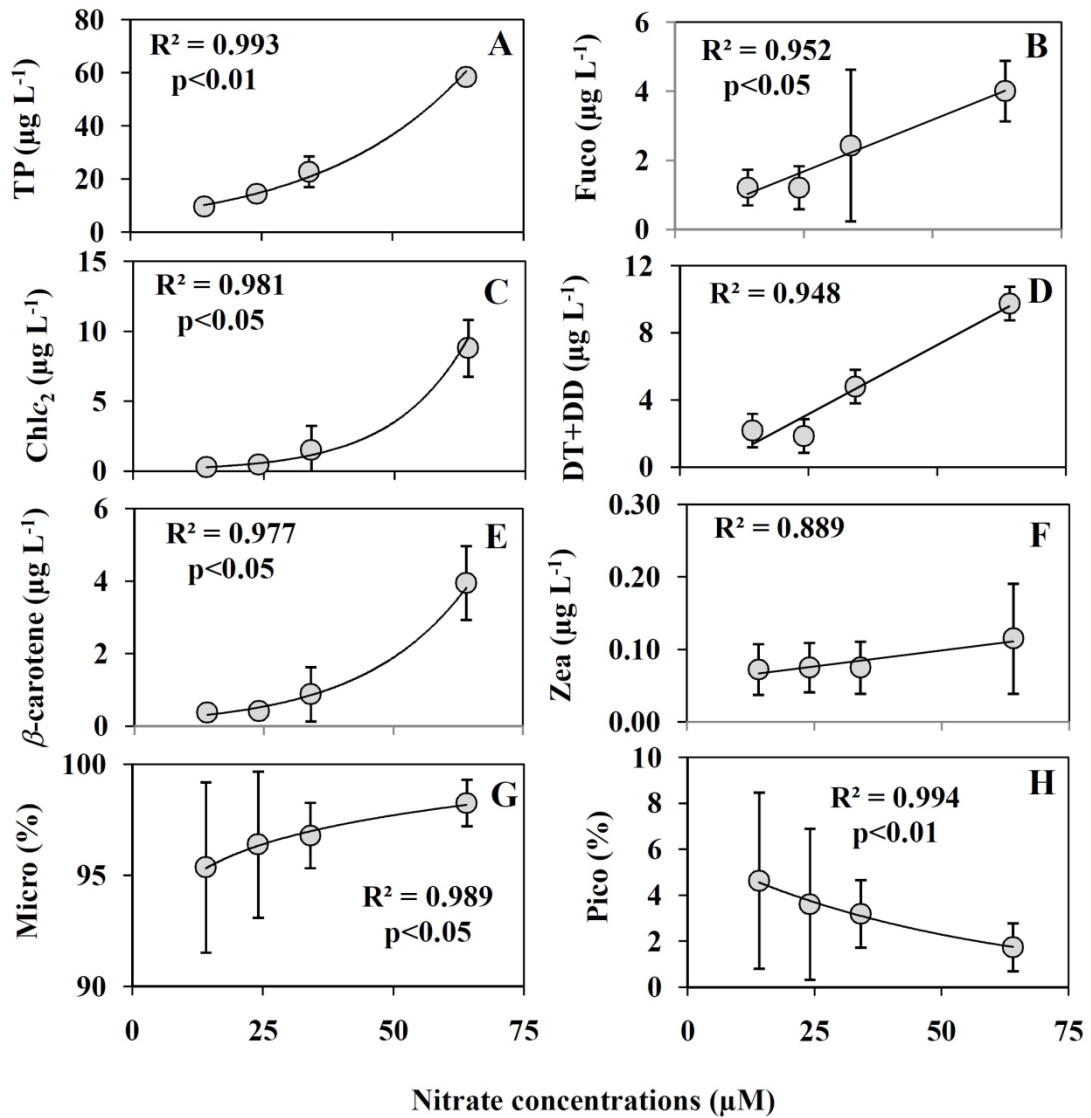


Figure 9: The concentrations of a) total pigment (TP); b) fucoxanthin; c) Chlc₂; d) diatoxanthin+diadinoxanthin; e) β-carotene; f) zeaxanthin detected in the HPLC analysis of the pigment extracts of Exp-III. The relative % of g) microphytoplankton (represents diatom) and h) picophytoplankton (mostly cynaobacteria) calculated based on the diagnostic pigment concentrations detected in HPLC pigment analysis (values = average±SD; n =2).

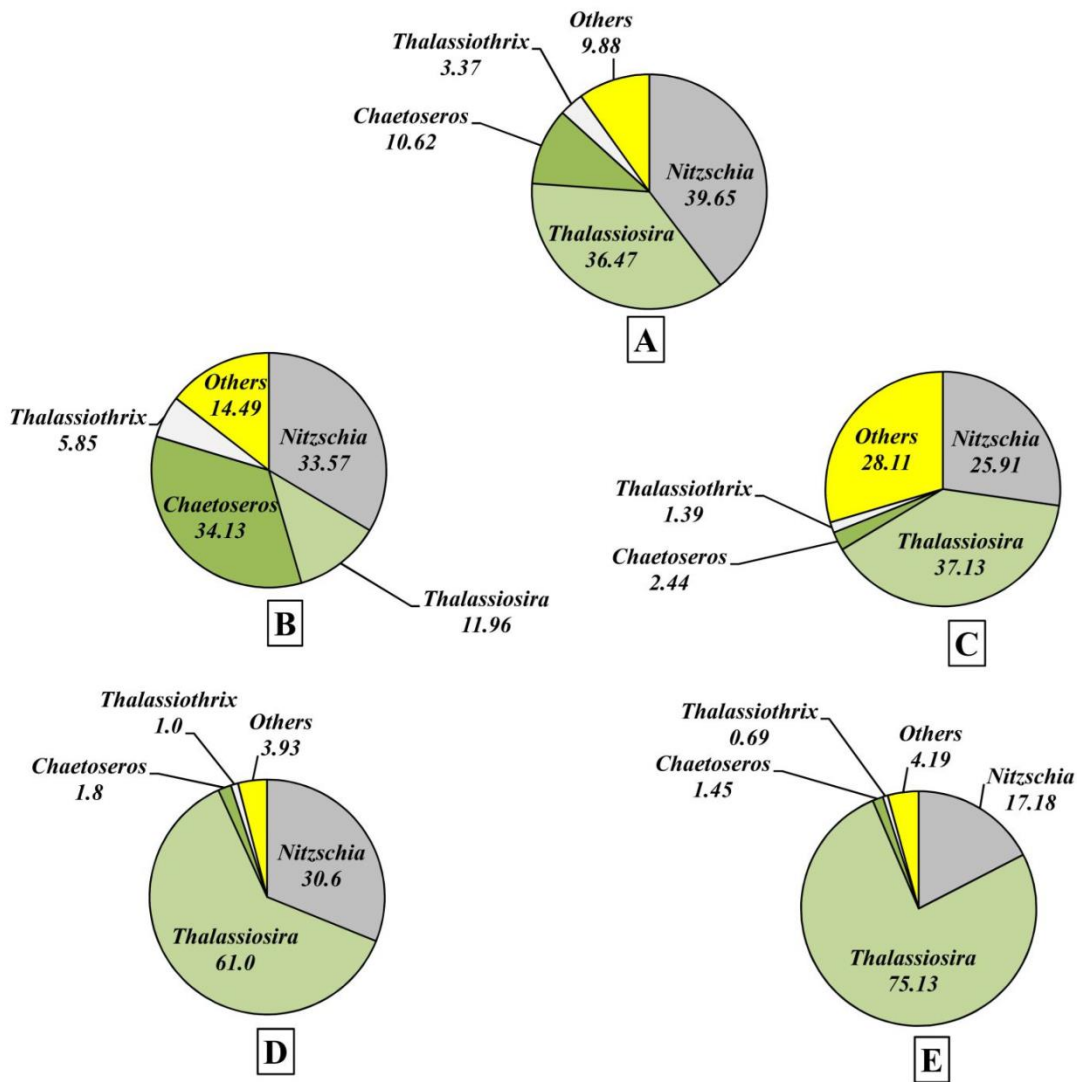


Figure 10: The relative abundance of different diatom species from the Exp-III under different nitrate addition. a) The community composition of the initial phytoplankton stock; the community compositions at the b) 14μM; c) 24 μM; d) 34 μM and e) 64 μM nitrate levels.

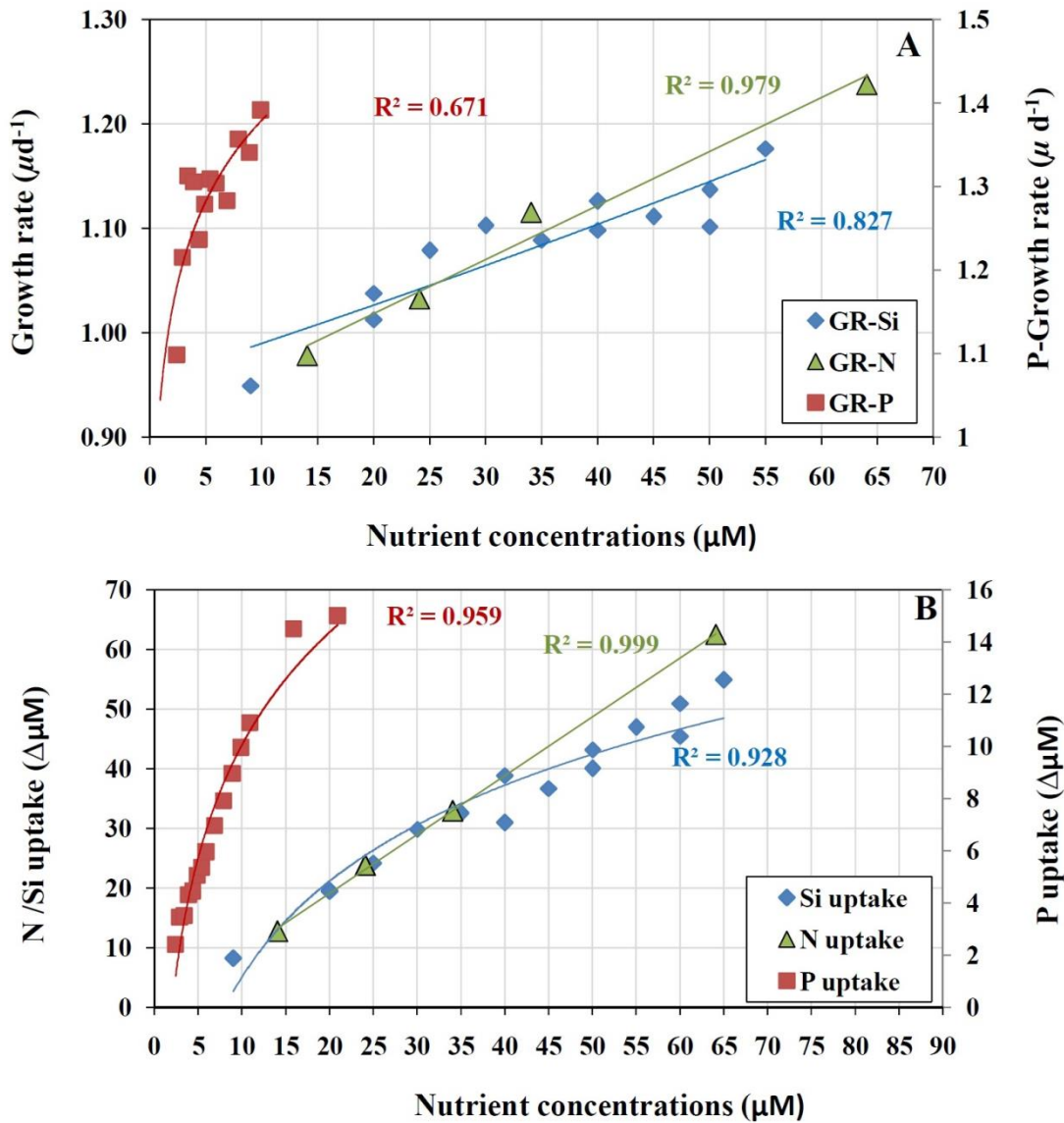


Figure 11: Growth and nutrient uptake rates (Δ) from all experiments. The first panel represents (a) the maximum growth rates for all three nutrients up to the growth saturating nutrient concentrations. The second panel represents (b) the luxury uptake for all nutrients after the growth saturating phase before reaching the plateau. Three different color codes have been used to denote P (red), N (green) and Si (blue).